

1 **Recent Advances in Nature-Inspired Solutions for Ground Engineering (NiSE)**

Deleted:

2 Arya Assadi-Langroudi<sup>1,\*</sup>; Brendan C. O'Kelly<sup>2</sup>; Daniel Barreto<sup>3</sup>; Federica Cotecchia<sup>4</sup>; Henry Dicks<sup>5</sup>;  
3 Abdullah Ekinci<sup>6</sup>; Fernando Estéfan T. Garcia<sup>7</sup>; Michael Harbottle<sup>8</sup>; Vito Tagarelli<sup>4</sup>; Ian Jefferson<sup>9</sup>;  
4 Pooneh Maghoul<sup>10</sup>; Enrico Masoero<sup>11</sup>; Gráinne El Mountassir<sup>12</sup>; Balasingam Muhunthan<sup>13</sup>; Xueyu  
5 Geng<sup>14</sup>; Soheil Ghadr<sup>15</sup>; Mehdi Mirzababaei<sup>16</sup>; Helen Mitrani<sup>11</sup>; Leon van Paassen<sup>17</sup>

Deleted: h

6 <sup>1,\*</sup> Department of Engineering and Construction, University of East London, England, E16 2RD, UK.

7 ORCID <https://orcid.org/0000-0003-3657-552X> [Corresponding Author –

8 [A.AssadiLangroudi@uel.ac.uk](mailto:A.AssadiLangroudi@uel.ac.uk)]

9 <sup>2</sup> Department of Civil, Structural and Environmental Engineering, Trinity College Dublin, Dublin, D02

10 PN40, Ireland. ORCID <https://orcid.org/0000-0002-1343-4428>

11 <sup>3</sup> Edinburgh Napier University, Edinburgh, Scotland, UK

12 <sup>4</sup> Politecnico di Bari, Bari, Italy

13 <sup>5</sup> University of Leeds, Leeds, England, UK

14 <sup>6</sup> Middle East Technical University, Güzelyurt, Cyprus

15 <sup>7</sup> University of Michigan, Ann Arbor, USA

16 <sup>8</sup> Cardiff University, Cardiff, Wales, UK

17 <sup>9</sup> University of Birmingham, Birmingham, England, UK

18 <sup>10</sup> University of Manitoba, Winnipeg, Canada

19 <sup>11</sup> Newcastle University, Newcastle, England, UK

20 <sup>12</sup> University of Strathclyde, Glasgow, Scotland, UK

21 <sup>13</sup> Washington State University, Pullman, USA

22 <sup>14</sup> Warwick University, Coventry, England, UK

23 <sup>15</sup> National Cheng Kung University, Tainan, Taiwan

24 <sup>16</sup> Central Queensland University, Melbourne, Australia

25 <sup>17</sup> Arizona State University, Phoenix, USA

26

27

28 *For potential publication in International Journal of Geosynthetics and Ground Engineering*

29 <https://www.springer.com/journal/40891> ; <https://www.scopus.com/sourceid/21100913564#tabs=1>

30

31

32

35 **Abstract**

36 The ground is a natural grand system; it is composed of myriad constituents that aggregate to form  
37 several geologic and biogenic systems. These systems operate independently and interplay  
38 harmoniously via important networked structures over multiple spatial and temporal scales. This  
39 paper presents arguments and derivations couched by the authors, to first give a better understanding  
40 of these intertwined networked structures, and then to give an insight of why and how these can be  
41 imitated to develop a new generation of nature-symbiotic ground engineering techniques. The paper  
42 draws on numerous recent advances made by the authors, and others, in imitating forms (e.g.,  
43 synthetic fibres that imitate plant roots), materials (e.g., living composite materials, or living soil that  
44 imitate fungi and microbes), generative processes (e.g., managed decomposition of construction  
45 rubble to mimic weathering of aragonites to calcites), and functions (e.g., recreating the self-healing,  
46 self-producing, and self-forming capacity of natural systems). Advances are reported in three  
47 categories of Materials, Models, and Methods (3Ms). A novel value-based appraisal tool is also  
48 presented, providing a means to vet the effectiveness of 3Ms as standalone units or in combinations.

49 **Keywords:** Biomimicry; Soil; Improvement; Self-heal; Natural.

50 **Declaration**

51

52 **Funding:** This paper is made available through contributions of authors to the NiSE1 Workshop, which  
53 was helped through financial assistance of the National Research Foundation, Department of Science  
54 and Technology South Africa, and The Royal Society UK, through the Newton Fund DST-NRF  
55 NFPF170627245562 grant.

56 **Conflicts of interest/Competing interests:** None.

57 **Availability of data and material:** None.

58 **Code availability:** Not Applicable.

59 **Ethics approval:** Not Applicable.

60 **Consent to participate:** Co-authors agree to participate in publication of this paper.

61 **Consent for publication:** Co-authors agree to participate in publication of this paper.

62 **Author's contribution statement:** AAL <sup>(1)</sup> steered the discussions among the team and has  
63 written up the paper. BCO <sup>(2)</sup> edited the paper and co-steered discussions among the team.  
64 DB <sup>(3)</sup>, FETG <sup>(7)</sup>, AE <sup>(6)</sup>, and MH <sup>(8)</sup> provided inputs on analytical methods. IJ <sup>(9)</sup> and AAL <sup>(1)</sup>  
65 developed the conceptual framework. HD <sup>(5)</sup> led, wrote and edited the philosophical  
66 backgrounds of NiSE. SG <sup>(15)</sup>, MM <sup>(16)</sup> and XG <sup>(14)</sup> fed in, and contributed to, discussions on  
67 nature-inspired materials and laboratory-scale methods. FC <sup>(4)</sup> and VT <sup>(4)</sup> led the field-scale  
68 methods. LVP <sup>(17)</sup>, HM <sup>(11)</sup>, BM <sup>(13)</sup>, GEM <sup>(12)</sup> led on, and fed into the bio-mediated methods.  
69 PM <sup>(10)</sup> contributed to multiple sections and offered a second round of editing. EM <sup>(11)</sup> led on  
70 meso-scale advanced models. All authors reviewed the paper and supported AAL <sup>(1)</sup> in getting  
71 the work to the presented state.

72

73

74

75

76

77

78

79

80

81

82

83

84

85

86

87

## 88 1. Introduction

### 89 1.1 Natural and Engineered Ground: Circularity and Man-made Disruptions

90 The ground is a grand system of systems. For provision of continual services, it deploys *mechanisms*  
91 that allow the constituting systems to interplay. Each system is made up of elements that are naturally  
92 adaptable, responsive, and constantly evolving. Systems have fractal properties at many levels. This  
93 means the characteristics of each system can be manifested in, or be predicted from, the properties  
94 of elements. Systems are self-healing, self-producing, and self-forming. This means elements in  
95 systems constantly evolve, adopt form and roles in response to environment, and re-establish  
96 functions that are disrupted in the natural erosive and stress environment. Collectively, these  
97 *constitutive properties* mark the fundamental difference between natural and engineered ground, as  
98 two different types of grand systems.

99 To better understand this difference, the critical transport infrastructure, taking London  
100 Underground (LU) as an example, may be considered as one type of an engineered grand system. The  
101 LU railway lines constitute of 300 m blocks, within which traffic is restricted to one train at any given  
102 time. The blocks are kept clear for passing trains through a 'signalling' technology. Trains stop running  
103 when signals fail. This can happen due to a short circuit in a wet day (causing disruption in how systems  
104 interact or *mechanisms*), but also occurs due to failure of any small component of the track (failure of  
105 systems or their components). In this respect, failure in any one system – in conventional engineered  
106 grand systems – will probably have cascading ramifications. On the other side of spectrum, take dune  
107 sand as an example of a natural grand system. Overall, dune sand can be inherently breakable. In the  
108 natural stress environment, groups of certain sized particles split to finer size. The breakage output  
109 appears in two forms, that is either aggregates of 'closely interlocked' and 'welded' fines, or a 'sea' of  
110 detached fines. Among the fines are mature particles that survive further breakage, and defected  
111 particles that break further into finer fragments. Both mature and defected particles adopt certain  
112 signature shapes. Among the aggregates are clast-like units that only break under large or anisotropic  
113 loads, or a prolonged course of stressing and through the mechanism of fatigue fracturing. Looser  
114 aggregates break into fines, some independent, and some in form of smaller sized aggregates. In this,  
115 the sorting, grading and mode-size distribution of sand are varied qualities. The structure is self-  
116 producing and self-healing, certain pronounced mode sizes continuously disappearing and  
117 reappearing. The components constantly evolve – in size and shape. During their lifetimes,  
118 components play various roles (e.g., as welding agents in clast-like aggregates that trap, compress and  
119 split fines into finer fragments, or as individual fines breaking into finer fractions), in response to  
120 environmental actions. Components have a capacity of re-establishing functions that are disrupted,

121 and their constant evolution have fractal characteristics [1-2]. Owing to these varied and fractal  
122 features, failure of components (e.g., breakage of particles) would not disrupt the overall behaviour  
123 of the grand system.

124 Traditional (or conventional) engineered ground in the built environment context is a product  
125 of mechanical or chemical densification, with an often predominant mission of enhancing stiffness,  
126 and stress at steady states, at the cost of filling and compacting void spaces, and replacing air, water  
127 and microorganisms with calcium-based cements and alike. This transforms the natural ground into a  
128 self-standing (e.g., for cuttings), impermeable (to line buried wastes or control groundwater), strong  
129 and stiff (to bear superstructure loads) medium. However, this causes disruption to the  
130 biogeochemical cycles and self-forming, self-healing capacities of structures which are reliant on soils'  
131 intertwining pore network and driven by interaction amongst frame and bonding elements, and also  
132 the living organisms present.

133

#### 134 **1.2 Biomimicry: A Philosophical Perspective**

135 At a general theoretical level, biomimetic or bio-inspired innovation involves observing natural  
136 systems, abstracting traits from those systems, and transferring those abstracted traits into  
137 engineering or design solutions [3]. While there exist numerous typologies covering the different basic  
138 types of traits that may be abstracted from nature [4-5], the ideal typology would be economical, such  
139 that there are as few basic traits as possible, comprehensive, such that all the basic traits are included,  
140 and coherent, such that the different traits fit together without overlapping, like the pieces of a jigsaw.  
141 Just such a typology may be established through drawing on Aristotle's doctrine of the four causes (see  
142 pp. 38-41 in [6]). From this perspective, there are only four basic types of traits we may abstract from  
143 nature and thereafter take as model: namely, forms, materials, generative processes, and functions.

144 In the case of the traits, we may abstract forms from the ground (understood as a natural  
145 system), such as rod-shaped, fibrous aragonite calcium carbonate in natural form, or as product of  
146 carbon sequestration in Ca-Mg silicates from construction and demolition wastes. As for the materials,  
147 they may be either abiotic (e.g., recycled and upcycled fibres, soils, etc.) or biotic (e.g., plants, micro-  
148 organisms, worms). Drawing on Aristotle, the concept of generative process covers both the  
149 generation of entities (producing) and the generation of effects (effecting) – see Ibid pp.39. In the case  
150 of the ground, examples of the former include bio-mineralization and humus formation, and examples  
151 of the latter include carbon sequestration and water infiltration. As for the functions, these are the  
152 roles the natural system plays in larger systems of which it is but a part. In the case of the ground, they  
153 may include such phenomena as habitat construction, climate regulation, erosion prevention, and soil

154 stabilization. They differ from generative processes inasmuch as the same function may potentially be  
155 achieved using different processes; one may abstract from nature a specific function (e.g., soil  
156 stabilization) but realize it in quite different ways (e.g., mechanical as opposed to biological  
157 stabilization techniques).

158         The traits abstracted from nature may also be imitated at differing levels of abstraction. One  
159 may, for example, imitate the precise way that a specific species of plant stabilizes the soil. But one  
160 may also imitate the general principle – abstractable from any number of different natural ground  
161 systems – of stabilizing the soil using plant roots. As a general rule, the difference between biomimetics  
162 and bio-inspiration lies precisely in the fact that bio-inspiration works at higher levels of abstraction; it  
163 is general principles and techniques related to such desirable functions as soil stabilization, carbon  
164 sequestration, habitat provision, and so on, that are abstracted from nature, rather than concrete  
165 models derived from a specific natural system.

166         Lastly, it is also important to note that biomimetic and bio-inspired designs involve a further  
167 feature one may call “composition”. If, as Aristotle maintains, both natural and design systems may be  
168 analysed in terms of forms, materials, generative processes, and functions, and if biomimetic or bio-  
169 inspired engineering involves abstracting these traits from natural systems and transferring them over  
170 to artificial systems, it is also true that one may abstract traits from different natural systems, and, in  
171 some cases at least, combine them with artificial traits devised by humans. An artificially engineered  
172 ground system may, for example, imitate both the forms and the functions of a natural ground system,  
173 while using artificial materials and while being generated using artificial processes. In such an instance,  
174 the artificial system would have been composed by joining together forms and functions abstracted  
175 from nature with materials and generative processes devised by humans. But, provided at least one  
176 trait has been imitated from nature for purposes of imitation, the artificial design may nevertheless be  
177 characterized as biomimetic or bio-inspired.

178         Drawing on this understanding of the process of biomimetic and bio-inspired innovation, the  
179 present contribution will present numerous advances in soil engineering that imitate – at varying levels  
180 of abstraction and in the context of varied compositions – at least one basic trait, whether form (e.g.,  
181 synthetic virgin fibres that imitate plant roots in tying together loose soil particles), materials (e.g.,  
182 living composite materials or living soil that imitate fungi and microbes), generative processes (e.g.,  
183 managed decomposition of construction rubble inspired by geological transformation of aragonites to  
184 calcites – e.g., [7]), and functions (e.g., recreating the self-healing capacity of natural systems in the  
185 form of responsive materials).

186

### 187 **1.3 Rethought Deliverables in Ground Engineering**

188 Given the dual nature of engineered ground as, on the one hand, the cause of disordered ground  
189 ecosystem and, on the other, the stabilised bedding for earth structures and therefore the integral  
190 constituent of the built environment, it becomes a matter of urgency to ask whether there can be a  
191 generation of technologies, and by extension a rethought suite of materials, for preserving systems  
192 that underpin and service its natural functions. Ideally, engineering interventions need to transform  
193 the natural ground into a medium that continuously interplays with the environment around, adapts  
194 itself to changing weather, captures, conveys and retains precipitation waters, supports flora and  
195 fauna, stores and locks carbon, captures aerosols, eradicates dust efflux into air, absorbs contaminants  
196 and fixates buried domestic, rubble and demolition wastes and construction rubble to offer stability  
197 to subsurface and surface structures. The deliverables collectively shape a new way of thinking,  
198 '*primum non nocere*', or *first do no harm* [then do some good]. Engineered ground should ideally retain  
199 its original fractal characteristics, double-porosity quality (in granular soils) and structure-dependent  
200 behaviour, self-healing capabilities and mineralisation in response to fatigue and entropy. This ideal  
201 engineered ground is illustrated in Figure 1a, in the context of NiSE, short for Nature-inspired  
202 Solutions for ground Engineering.

203

#### 204 **1.4 NiSE – the Framework**

205 The NiSE deliverables are used to develop an adaptability indicator system and assessment method  
206 for evaluating different stabilising materials (and structures that evolve from the introduction of such  
207 materials to soil). Figure 1b presents a suite of indicators, or performance criteria, as well as a traffic-  
208 light scoring system that indicates the performance of materials based on the adaptation of the NiSE  
209 initiative. Indicators are deliberately without weightings to avoid subjectivity and to allow the model  
210 to be deployed globally and across multiple sectors and disciplines. Figure 1b is the blueprint of the  
211 NiSE initiative and provides a potential chance to be utilised as a value-based decision support  
212 framework for emerging ground engineering techniques. The five-point scoring scale is applied to each  
213 material in three primary categories of processes, forms and functions. The cumulative score for each  
214 material is a quantitative measure of a technique's impact within the NiSE context.

215

216 **Fig. 1** (a) NiSE five principal aims and interlinked deliverables; (b) NiSE deliverables as indicators of  
217 materials' performance, measured by a traffic-light scoring system: the framework can be applied to  
218 candidate stabilising materials in any project

219

220 The principal objectives of this paper is to collate latest advances in materials, methods and  
221 models that underpin these novel ground engineering interventions, to discuss their development and  
222 deployment within the biomimetic or bio-inspired innovations context, and their common  
223 deliverables: (1) preserved permeability and porosity, (2) balanced water retention and conveyance  
224 capacity, (3) durability in the face of low-order cyclic, transient or extreme-but-one-off actions  
225 (thermo-hydro-chemo-mechanical), (4) enhanced strength, stiffness and particularly small-strain  
226 stiffness, (5) enhanced steady states (quasi-steady state, ultimate steady state, phase transformation,  
227 critical state) and relaxed flow potential, (6) enhanced resilience in the face of extreme events, (7)  
228 adaptability to wider loading environment: hydrodynamic, cyclic, and anisotropic.

229

## 230 **2. Advances in Models and Methods**

231 The overall vision – within the context of NiSE – is to explore prospects for developing and deploying  
232 models and methods that enable capturing the behaviour of the porous multimodal soil medium, and  
233 for developing mediated soil materials that are inspired by or imitate nature.

### 234 **2.1 Soils and Particulate Matters Alike**

235 Models and methods vary across the spectrum of scales.

236 For clays with a median sub-2 $\mu$ m particle size, the flat platy shape of particles, high ratio of  
237 surface area to volume, and surface charges influence clay behaviour. For soft clays, in particular,  
238 accurate understanding of complex soil behaviour is possible at nanoscale and is paramount to  
239 admissible serviceability of structures, slopes, and earthen transport-infrastructure embankments, to  
240 name a few. At the nanometre scale, rigorous solutions to the underlying physics are possible and can  
241 be fully predicted. In fact, innovation is created at nanoscale. Molecular dynamics (MD) simulation is  
242 an example of nanoscale techniques that are used to explore the interaction between colloidal clay  
243 nano-platelets, their orientation and inherent anisotropy. The impacts of nanoscale innovations are  
244 deployed to develop micro-scale models, such as soil constitutive models. However, for such transition  
245 from nano- to micro-scale and ‘upscaling’, the behaviour of material needs to be simulated at an  
246 intermediate range of scale, broadly referred to as the meso-scale. Less established simulation  
247 methods are available at mesoscale. An inherent challenge to mesoscale simulation is the hardship of  
248 simulating long timescale (or slow) processes that may originate in such intermediate scales, like  
249 creep, fatigue, reaction rates and hydration. In other words, it is incredibly hard to model large  
250 timescales in small length scales [8]. Mesoscale models then inform microscale models, such as  
251 constitutive soil models, which are then extrapolated to engineering properties and capitalised for the



252 benefit of geotechnical and petroleum engineering applications. The thermodynamic perturbation  
253 method is gaining interest at mesoscale [9-10]. Alongside with MD simulation, the two methods  
254 combined are offering a chance to study interactions of multiple platelets with varied orientation (Fig.  
255 2), and a fresh insight into clay platelet arrangements – hence clay microstructure, aggregation under  
256 progressive pressure, and evolution of elastic stiffness and anisotropy with size of platelets.

257 Moving upwards along the scale and for sands, the surface area becomes small relative to the overall  
258 volume or mass of the particles, hence gravitational effects become more significant. The overall  
259 behaviour of the material for sands is insignificantly influenced by surface interaction and charges.  
260 Instead, the overall behaviour is influenced by the variety of particle shapes, size, sorting, and surface  
261 topology that can be as complicated as the topology of mountains. Significance of sand behaviour  
262 manifests in consequences of its problematic behaviours, including softening, flow and liquefaction.  
263 Examples of liquefaction ramifications include the wide-scale destructions in the Marina District, San  
264 Francisco, after the 1989 Loma Prieta Earthquake, in Onahama Port, Japan, and in Shortland Street in  
265 the suburb of Aranui, New Zealand, in 2011. The “Tesco” Tunnel collapse in June 2005 in London, UK,  
266 that incurred an estimated cost of £8.5 million is another notorious example. More recently, in January  
267 2019, the failure of Minas Gerais tailing dam in Brazil claimed 157 lives and showed the catastrophic  
268 significance of problematic sand behaviour.

269 Understanding how to work with soil has consequences, both in terms of natural hazards that are  
270 stemmed from soil’s highly complicated behaviour, and in terms of urban environment and  
271 construction of surface and subsurface structures that are surrounded with soil. It is highly  
272 advantageous to draw in expertise from other areas and disciplines in developing the understanding  
273 of soil, and its inherently complicated behaviour that is also dependent on the environment. These  
274 include research in particuology, powder technology, pharmaceutical sciences, and food and process  
275 engineering. A good example is the recent studies on fragmentation of infant milk agglomerated  
276 powder during transportation, including how inter-particle collisions play more significant role relative  
277 to particle-wall impacts during transportation (Fig. 3), and lessons for understanding soil particle  
278 crushing [11]. Another engineering discipline that can better shape knowledge of soil at fundamental  
279 level is metallurgy. An example is recent advances of in-situ synchrotron radiography, discrete  
280 element method (DEM) simulation and thermographic imaging (Fig. 4) that show the resemblance of  
281 semi-solid alloys to granular materials. In this context, [12] brought concepts of critical-state soil  
282 mechanics (CSSM) and shear-induced dilatancy that occurs in dense sands into the metallurgy  
283 discipline. They showed an improved understanding of dilatancy – this assisted in identifying weak  
284 zones in semi-solid metals that are used to cast mechanical components. More recently, [13] adopted  
285 the CSSM framework for interpretation of triaxial shear data of semi-solid alloy and reported

286 similarities to soils in terms of the pressure-dependent flow stress and pressure-dependent volumetric  
287 response.

288

289 **Fig. 2** Qualitative picture of aggregation during MD simulations; Clay platelets' orientations according  
290 to the  $\varphi$  angle ( $0^\circ$  representing alignment of normal vector of platelets with the z axis) [14]

291

292 **Fig. 3** Simulation of uniaxial compression of highly porous particulate matters through importing the  
293 "diffusion-limited aggregation" algorithm into 3D DEM software package PFC3D [11]

294

295 **Fig. 4** Left: aluminium die casting and significance of identifying areas of potential weakness [15];  
296 Right: coupled LBM-DEM simulations and time-resolved synchrotron X-ray radiography applied to  
297 the study of complex stress-strain behaviour of globular Al-Cu alloys and links to critical-state soil  
298 mechanics [12]

299

## 300 **2.2 Challenges in Predicting the Behaviour of Soils**

301 An informed adoption of simulation and observation methods for soil needs an in-depth  
302 understanding of the difficulties in predicting the behaviour that arises from the fact that soil is a  
303 particulate material. A natural (not engineered) soil is generally inherently variable. This differentiates  
304 soil, as a material to work with, from most other engineering materials. It is intuitive to geotechnical  
305 engineers that soil strength is stress-dependent, and the extent of steady states depends on soil  
306 packing state. The non-linearity of stiffness and the fact that stiffness is also stress dependent are  
307 other phenomena intrinsic to a granular material and which make prediction of soil behaviour more  
308 complicated. However, this is not limited to natural soils, but arises from particle-scale interactions.  
309 As the contact force increases due to an increase in the confining pressure, the contact area increases  
310 and hence the stiffness. Furthermore, stiffness progressively degrades with increasing strain, a fact  
311 that arises from the particulate nature of soils. Other challenges of working with soil include the  
312 hysteresis under cyclic loading, strain softening and localization, anisotropy and significance of  
313 intermediate principal stress, phase transformation under undrained loading, non-coaxiality [14], and  
314 temperature-dependent properties [16].

315

## 316 **2.3 Models, Simulations and Methods**

317 Many of the biggest challenges regarding ground engineering are associated with fundamental  
318 behaviours of soils. Taking coarse soils as an example, these include grain-to-grain interactions, the

319 influence of pore space, and dilatancy. Particle-continuum duality of soils suggests that all behaviours  
320 which we can model at the macro-scale stem from the physics at the micro- or granular-scale. The  
321 ground, which we see as continuous from afar, is fundamentally composed of distinct grains separated  
322 by pore space. Tools such as micro-computed tomography ( $\mu$ CT) and scanning electron microscopy  
323 (SEM) that facilitate visualization of the particulate, or granular, nature of soils allow us to visualize  
324 the efficacy of different ground improvement techniques at the micro-scale. For example, [17] used  
325 SEM coupled with energy dispersive X-ray spectroscopy as a tool for evaluating the capability of coal  
326 ash treated with microbial-induced calcium carbonate precipitate to minimize leachability of trace  
327 elements into groundwater sources. Other imaging tools, notably X-ray  $\mu$ CT, facilitate visualization of  
328 grain movements and interactions in three dimensions (3D) during shearing (e.g., [18-20]). This section  
329 will explore advances in numerical and observation methods and technologies, and how these are  
330 offering novel insights into soil as a complex particulate matter.

331

### 332 **2.3.1 Advances in Simulations**

333 Modelling and simulation, in the context of NiSE, aims for betterment of our understanding of the  
334 origin of material behaviours, extrapolating long-term behaviours, designing composition and  
335 microstructures, in-silico design of complex materials, and new ways to minimise infrastructure  
336 degradation and maintenance, as well as to increase resilience.

#### 337 ***Nanoscale: Molecular Modelling***

338 Simulations at nanoscale offer an understanding of atomistic-level geochemical processes required  
339 for identification of mechanisms and properties that control the thermodynamics and kinetics of soil  
340 in its natural, weathered and mediated forms. In the context of NiSE, nanoscale modelling provides a  
341 broad range of opportunities, including predication of dissolution, precipitation and reprecipitation  
342 rate of biomimetic and biogenic materials (e.g., biopolymers and how these interact with  
343 phyllosilicates in the short- and long-terms), biocrusts formation, evolution and degradation, and  
344 formation of Calcium Silicate Hydrate (C-S-H) in deprotonated clays. These provide the basis for  
345 prediction of complex materials' behaviour. Noteworthy among several textbooks that provide  
346 comprehensive reviews of molecular modelling methods is [21]. Molecular mechanics is a common  
347 thread and includes a range of techniques, including MD simulation, which has received considerable  
348 interest in the geoscience discipline. The MD technique computes forces, based on Newtonian physics,  
349 to evaluate the time evolution of a system on the time scale of pico- and nano-seconds. Recent uses  
350 of atomistic simulations in the context of NiSE include development and testing of hybrid

351 nanocomposites of C-S-H with organic compounds, and also composites (from intercalation of  
 352 biomediated or bioinspired materials into clays [22]), modelling the interactions between calcite and  
 353 organic matters (kerogen) within the soil pore phase and implications on calcite-kerogen binding [23],  
 354 and validating efficiency of plant-microbial combined bioremediation of PCN-contaminated soils [24].  
 355 Figure 5 presents examples of molecular simulations. In Fig. 5a, outputs from MD analysis are  
 356 presented, aimed at determining chemical interactions between kerogen and calcite within the  
 357 nanoscale voids of a porous soil, and measurement of interparticle forces. Figure 5b presents outputs  
 358 of MD analysis using Large-scale Atomic/Molecular Massively Parallel Simulator (LAMMPS) package  
 359 to study creep deformation of C-S-H. The method simulates the artificial aging observed in granular  
 360 materials subjected to vibrations. Figs. 5c,d show crystal structure and forcefield for a complex  
 361 multibody nano-silica (NS)–kaolinite–sulphates system. Synthetic NS replicates weathered quartz in  
 362 the sedimentary environment and, hence, in the context of NiSE, counts as a bio-inspired material.  
 363 Figure 5c illustrates the process of silicatisation of kaolinite (soft clay), where orthosilicate anions  
 364 share electron with the edge oxygen atom of aluminium octahedral unit to form strong Si-O-Si-O rings  
 365 [25]. Figure 5d illustrates the NS–kaolinite–sulphates system determined by the summation of all  
 366 energy interactions over all atoms of the system [25], and formation of Al-HO-Si-O-Si-O-M-Anion and  
 367 Al-HO-Anion-O-Al-O rings that assist retaining the intra-lattice pore spaces (an objective in NiSE).

368

369 **Fig. 5** Examples of molecular modelling and their application in geomechanics in the context of NiSE:  
 370 (a) molecular dynamics (MD) simulation of minimized and equilibrated kerogen–calcite system that is  
 371 useful for calculating the non-bonded interactions between the organic matter and calcite in porous  
 372 soils ([23] – with some modifications); (b) variation of shear strain (creep) with potential energy  
 373 against number of loading/unloading cycles in C-S-H [26]; (c-d) crystal structure and forcefield for a  
 374 complex multi-body NS–kaolinite–sulphates system [25]

375

### 376 **Mesoscale: Particle-based Simulations**

377 Particle-based simulation, as one of the many possible bespoke mesoscale simulation techniques,  
 378 offers upscaling from molecular simulations. The technique is particularly useful in determining the  
 379 behaviour of aggregated nanoparticles of various shapes and morphologies – many kinds to be  
 380 described later in this contribution – after aggregation. The technique allows extracting properties  
 381 from the nanoscale and upscaling these into actions at micro-scale. For example, the method can  
 382 average out interaction potential between molecules into potentials of mean force between particles,  
 383 thereby allowing an insight into static and dynamic mechanical behaviours of aggregated  
 384 nanoparticles. The technique has gained much recent interest and is being refined to avail achieving

385 long timescales, and also to accommodate less simplified and more rigorous chemical kinetics and  
386 reactions [8]. The latter allows better imitation of formation and degradation of materials.

387 Three examples of mesoscale simulations, within the context of NiSE, are the application of  
388 chemo-mechanics mesoscale simulation to study the rate and mechanisms of agglomeration of  
389 nanoparticles and C-S-H precipitation [27], the recent study of self-organisation of minerals and  
390 bacterial activities during MICP – microbial-induced calcite precipitation [28], and the recent use of  
391 Kinetic Monte Carlo (KMC) to simulate removal and insertion of particles into aggregation of particles  
392 (connected together with an effective interaction potential) in order to model dissolution and  
393 precipitation [29]. The latter work marks integration of chemical-transformations in particle-based  
394 simulations and could be of interest to researchers studying bio-mineralisation and self-healing at  
395 mesoscale, and also carbon sequestration into silicates and carbonates.

396

#### 397 ***Microscale: Discrete Element Method (DEM)***

398 The Discrete Element Method (DEM) continues to gain popularity as a strong tool in capturing,  
399 arguably, all challenges in predicting soil behaviour [14] at the micro-scale. DEM idealises soil grains  
400 with geometries that can be described analytically, allowing creation of contact/rheological models.  
401 In DEM simulations, assemblies of spheres are most common, where the spheres are rigid and allowed  
402 to overlap by a small amount. The overlap is then used to calculate the magnitude of the normal  
403 interparticle force, through normal springs that can be linear or non-linear. In the shear directions,  
404 particles are allowed relative movement to mobilise shear force, which may come up to a threshold  
405 value at which particles begin to slide relative to each other. In this, the DEM method allows contacts  
406 to form and to break. DEM is an *abstraction of reality* and a method that allows creating virtual  
407 samples of soil (sand), running simulations, and measuring the forces between individual particles.  
408 Despite the popularity of this method in the geomechanics discipline, the big limitation of DEM is the  
409 number of particles that can be considered. For instance, a 1 cm<sup>3</sup> box of sand contains approximately  
410 150,000 particles (of uniform size and 200 µm median diameter). The majority of simulations  
411 published in leading geomechanics journals report findings from simulations using less than 150,000  
412 particles in response to computational costs — that is, hardly a reasonable representative element  
413 volume [30]. This can negatively impact the boundary effects in materials behaviour. The constraint  
414 has been partially relaxed in recent years through using novel codes and high-performance computing.

415 An important example of DEM advantage in understanding the behaviour of open-structured  
416 particulate matters is the impacting of fines fraction on seepage-induced boiling and flow (static

417 liquefaction) potential of porous granular soils. Hydromechanical soil properties, such as air entry  
 418 value, collapsibility, and potential of flow, are associated with the overall layout of interconnected  
 419 micro ( $<0.001 \mu\text{m}$ ), meso ( $0.001$  to  $0.25 \mu\text{m}$  and  $0.3$  to  $1.5 \mu\text{m}$ ) and macro ( $2$  to  $20 \mu\text{m}$ ) voids, and the  
 420 degree to which these contain fines at any one time [31-32]. These 'fractions' of void spaces control  
 421 soil packing states [33]. For example, a Random Loose Packing (RLP) that typically occurs at void ratio  
 422 above  $0.6$  changes to Random Close Packing (RCP) as void ratio reduces to typically between  $0.5$  and  
 423  $0.6$ . Under constant effective stress, such change in void ratio can occur as a result of fines migration.  
 424 Changes in void ratio can also be produced as a result of mineral dissolution and/or biodegradation  
 425 [34]. In the context of NiSE, fines can be additive nuclei. [35] found a threshold  $30$  to  $40\%$  fines content,  
 426 at which point idealised skeletal and fine void ratios reach to a similar value [32]. This marks a state  
 427 where an interconnected homogeneous network of pores form and the soil reaches the phase  
 428 transformation stress state (static flow), which is an unwelcomed condition (Fig. 6). DEM simulation  
 429 allows quantification of the degree to which fines carry effective stress and their ability to move  
 430 through the pore network (Fig. 7 – [36]).

431

#### 432 **Challenges of DEM**

433 One of the greatest challenges in numerical simulation of granular materials and soils is the number  
 434 of grains in a simulation. A standard triaxial test sample of cohesionless sand could have millions of  
 435 individual grains, which is a prohibitive amount for a single-core computer. Inclusion of complex grain  
 436 morphologies increases the computational demands of a single simulation. Even with simplifications  
 437 in terms of larger grain sizes and idealized grain shapes, simulations of boundary-value problems  
 438 involving granular materials requires advanced computing tools. For example, earthquake surface-  
 439 fault rupture has been simulated with hundreds of thousands of grains with multi-core processing  
 440 (e.g., [37-38]) and with graphics processing units (e.g., [39]). Upscaling the number of grains to the  
 441 millions is achievable with high performance computing (e.g., [40-41]). As processing units and  
 442 computational technologies improve, increasingly complex simulations of soil behaviour become  
 443 possible, thus facilitating deeper understanding of soil behaviour at the granular-scale.

444

445 **Fig. 6** For threshold fines content of  $30$  to  $40\%$ : (a) maximum static flow potential [45]; (b) equal  
 446 idealised micro- and macro-void ratios [35]; (c) changing fabric from RLP to RCP as fines content  
 447 increases beyond the  $30$  to  $40\%$  threshold [32 – with permission from ASCE]; (d) maximum  
 448 liquefaction risk [35]

449

450 **Fig. 7** DEM–DFD coupled simulation for a gap-graded material showing the greater ability of fines to  
451 transmit effective stress through the pore network [36]

452

#### 453 ***Level-Set Discrete Element Method (LSDEM)***

454 In order to more fully understand soil behaviour at particle level, the contacts between grains and  
455 other materials must also be quantified. Except in the case of photoelastic materials, high-resolution  
456 imagery typically will not offer any information on the magnitude of forces that act between grains.  
457 Numerical modelling is necessary to quantify these contact forces in terms of contact orientation and  
458 contact force magnitude. DEMs are highly suited for contact force calculations based on Hooke's law  
459 for elastic springs. In particular, the level-set discrete element method (LSDEM, [42-43]) can capture  
460 the exact morphologies of grains observed in  $\mu$ CT images, as well as quantifying the contact forces  
461 acting between contacting grains. LSDEM coupled with  $\mu$ CT allows for the shapes and kinematics of  
462 the grains themselves, and the distribution of contact forces that exists within the granular matrix, to  
463 be quantified fully via one-to-one physical–numerical comparisons. Entire shear simulations are  
464 possible for complete analysis of CSSM within the shear band itself (e.g., [43]). Furthermore, more  
465 complex granular mechanics, such as grain fracturing and crushing, may be included to evaluate the  
466 critical state behaviour of soils at a wider range of stresses (e.g., [44]). This level of detail in simulations  
467 can improve soil constitutive models by providing a means of virtual laboratory testing.

468

#### 469 ***Critical State Soil Mechanics (CSSM) for Reinforced Soils***

470 [45] are among the few who have performed high pressure laboratory studies on fibre-sand mixtures  
471 and adopted a critical-state framework to describe their mechanical behaviour. [46] conducted  
472 dynamic and monotonic triaxial testing to study the behaviour of carbon-fibre-reinforced recycled  
473 concrete aggregates by focusing on the very small and large strain ranges. Authors reported that, at  
474 large strains, reinforced and unreinforced specimens showed comparative stress–strain response and  
475 volumetric behaviour with similar critical state parameters, the fibre-reinforced specimens having  
476 slightly higher critical state angle of shear strength. More recently, [47] utilised critical-state  
477 framework to compare the performance of polypropylene and rubber fibres in well-graded  
478 decomposed granite. In a similar study, [48] examined the effect of adding fibres to a completely  
479 decomposed granite (CDG) in the context of critical-state framework. They reported that while  
480 unreinforced CDG is sensitive to sample preparation, the reinforced soil is not sensitive to the method  
481 of material or sample preparation. It is evident from earlier studies that, until now, not many have  
482 attempted to investigate the CSSM for fibre-induced cohesive soils.

483

484 ***Soil constitutive models for reinforced soils***

485 Although several studies have been conducted on fibre-reinforced clays, little is known on the  
486 implications of in-situ compaction of cohesive material reinforced with fibres. [49] presented findings  
487 from a study of the compaction of clay peds and fibres, and the consequent creation of discontinuities  
488 in the contacts between clay peds and clay-peds-and-fibres.

489 In their extensive study of Lambeth group clay, [50] reported that a large amount of the  
490 formation comprises of largely unbedded, mottled silty clay and clay alone. They reported that during  
491 the deposition of the Lambeth group, fissures with polished and slickensided surfaces developed due  
492 to desiccation throughout seasonal changes in ground moisture. [50] also studied the effect of  
493 fissuring on compression behaviour of over-consolidated Lambeth group clay and showed that the  
494 compression response of tested specimens is highly dependent on fissures. In a later study, [51]  
495 reported that there are two state boundaries in London clay not subjected to previous shearing; that  
496 are the upper bound, defined by the peak failure envelope of the intact clay without fissures, and the  
497 lower bound given by the parameters defining the strength of the fissures.

498 London Clay belongs to a geological unit above the Lambeth Group and they have similar  
499 characteristics; however, the former has been deposited under a variable sea level, with sand lenses  
500 found when the sea level was shallow, causing the appearance of beaches. London Clay is highly over-  
501 consolidated, intensely fissured. [52] and [53] showed that the effective strength of London Clay with  
502 dull or shiny surface fissures exhibit a zero effective cohesion on fissured surfaces and an effective  
503 friction angle equal to the global soil substance of the intact material, whereas slickensided surfaces  
504 show an effective strength similar to the residual values. More recently, [54] studied the influence of  
505 the structure on the behaviour of London clay. They used the State Boundary Surface (SBS) concept,  
506 which is constructed from all the effective stress paths for normally consolidated clay, lightly  
507 consolidated clay, over-consolidated clay and heavily over-consolidated clay at different initial stress  
508 states and for different test conditions (drained and undrained), to identify the changes in structure.  
509 They stated that, in compression, the peak state of clay from different units plot significantly above  
510 the SBS from the reconstituted specimens (i.e., SBS\*) for isotropically consolidated samples; this was  
511 considered a feature of the natural structure of the clay. [54] discussed the implications of structure  
512 increasing with depth; this remains a matter of debate.

513 In a study on a similar highly fissured and structured clay, [55] reported that the SBS of the  
514 unfissured clay is larger than that of the reconstituted clay, while the SBS of a clay with a high fissure  
515 intensity is smaller than the same reconstituted clay. The authors further suggested that the intense  
516 fissuring degrades the mechanical properties of the clay, with respect to both the original unfissured



517 material and the reconstituted soil. [55] reported that the fissured material had fissures with matt  
518 surfaces, where the peak strength of the clay generally stayed above the critical state. Additionally,  
519 [55] and [56] found that due to the heavily sheared and slickenside-like nature of the surface of the  
520 scales, the peak strength of the natural soil is lower than the critical state of the reconstituted soil.

521

### 522 **2.3.2 Advances in Spectroscopic Methods**

#### 523 ***Microcomputed Tomography ( $\mu$ CT)***

524 Microcomputed tomography offers high resolution images of sub-cores obtained from soil samples  
525 impregnate with epoxy resin. Figure 8 of this paper presents a rare and useful view of the  $\mu$ CT setup.  
526 The technique is continuously developing, not just in terms of the technology around acquiring the  
527 images, but in the ability to analyse the data that emerges.

528

529 **Fig. 8** Typical microcomputed tomography laboratory setup [14]

530

531 One important application of  $\mu$ CT in the context of NiSE is an improved understanding of double  
532 porosity, which is an intrinsic quality of bimodal soils (e.g., silty sands, mediated sands with  
533 nanomaterials). For bimodal soils, the size, geometry and evolution of constrictions or pore throats  
534 play pivotal roles in soil behaviour. Constrictions form the boundary between various scales of pore  
535 spaces and their reliable measurement, as a grain scale quality, can offer solution to a number of  
536 problems across the spectrum of porous particulate matters. A simple example is a recent study on  
537 Reigate sand from south of London, UK. Reigate sand has a self-supporting quality in open cuts, as  
538 particles naturally interlock and come together like jigsaw pieces. [57] conducted drained triaxial  
539 compression tests on intact and reconstituted samples at a constant 0.48 void ratio and under a  
540 constant 300 kPa cell pressure. They showed the intact material exhibits much more strain-softening  
541 and a higher peak strength than the reconstituted material. Using the  $\mu$ CT, they plotted contact index  
542 (i.e., the ratio of particle contact area to particle surface area) volumetric distribution for the two  
543 materials to quantify the contribution of contacts at particle scale. In addition to particle interlocking,  
544 constriction-size distribution (CSD) informs on how, and if, fines migration through the pore network  
545 modifies the contacts and impacts the skeletal stresses, suction, stiffness and steady states. For  
546 example, [58] used DEM to explore the impacting of particle-size distribution, relative density, and  
547 coefficient of uniformity of a suite of filters (i.e., porous granular soils) on CSD. They did not just test  
548 the viability of characteristic diameters in assessing filter retention capacity, but also the likelihood of

549 fines entrapment in narrow void throats. [59] exhibited the benefits of using network modelling  
550 (specifically the 'random walk' model) alongside CSD analysis to simulate the migration of fines  
551 through the soil pore network (Fig. 9). They used CSD data to confirm an earlier experimental finding  
552 of [60]; that is, the size of constrictions rather than topology of pores controls movement of fines  
553 through the pore network. In the context of NiSE, coupled  $\mu$ CT-DEM and  $\mu$ CT-Network Modelling assist  
554 in CSD-informed design of sands stabilised with a range of additives (from biopolymers to colloidal NS)  
555 in their originally high porosity. These also help a better understanding of seepage implications in  
556 flood defences and earth-based water reservoirs that are built with open-packed granular soils.

557

558 **Fig. 9** (a) Example of a network model for simulating the migration of base particles (e.g., clay, nano-  
559 stabilising agent, biopolymer nuclei) through the network, where the size of the edge of the network  
560 is determined from CSD, informed by  $\mu$ CT [59]; (b) Criteria, whether a base particle would move  
561 through the constriction, whether it would be trapped, and when it would be retained in the void  
562 space [59]; (c) An example of determining CSD as a function of 15% percentile of particle size [58]

563

564 The types of quantifiable interactions observed via  $\mu$ CT are not limited to soil grains. Complex  
565 biological processes that occur within the soil may also be visualized.  $\mu$ CT has been used to study the  
566 interaction of root growth with soil, and how root growth affects water uptake [61]. It has been used  
567 to study soil response due to ice formation in pores during freeze–thaw cycles [62]. These processes  
568 involve complex interactions with the grains themselves and the pore space among them; such  
569 interactions are practically impossible to be studied in absence of advanced imaging tools.  $\mu$ CT has  
570 also been used to study the interaction between rigid and soft particles in sand–rubber mixtures as a  
571 means for improving the properties/behaviour of sands [63]. Not only can the grains be visualized via  
572 processed X-ray images, but the kinematics and interactions of the grains can be quantified using  
573 software, such as the python-based Software for Practical Analysis of Materials (SPAM, [64]). This  
574 allows for shear-induced deformations to be visualized via grain rotations, grain displacements, shear  
575 strains, and volumetric strains, all in 3D.

576 The technique allows real-time capture of soil pore spaces in 3D under triaxial loading. For soils  
577 reinforced with fibres (natural or engineered), the technique offers a chance to capture, at sub-micron  
578 resolution, the evolving orientation and tortuosity of reinforcing fibrous matters within the spatial  
579 domain of soil under stress. This is valuable information, offering a unique chance to explain the, thus  
580 far, controversial anisotropic behaviour of fibre-reinforced soils [65-66]. In a quite innovative recent  
581 attempt, [67] managed to build and instate a miniature triaxial cell inside a Zeiss Xradia XRM520 Versa  
582 X-ray CT machine (Fig. 10). Typical outputs of CT results are illustrated in Figure 11.

583

584 **Fig. 10** Interior of the X-ray chamber accommodating miniature triaxial cell [70]

585

586 **Fig. 11** Reconstructed 3D greyscale images of triaxial mini-specimen at three axial strains and three  
587 views (XY, XZ and 3D), followed by spatial distribution of fibres and 3D distribution of fibre  
588 orientation and length at three axial strains (reproduced from [70])

589

590 Experiments using this technique are performed on “miniature” samples. However, the gain in  
591 resolution comes at the cost of losing the size of the representative elementary volume (REV). This  
592 has remained, thus far, a challenge.

593

#### 594 **Particle Image Velocimetry (PIV)**

595 The PIV technology – also known as digital image correlation (DIC) – allows non-invasive measurement  
596 of soil deformation by tracking the movement of individual soil particles through consecutive images  
597 captured from soil samples (test specimens). For example, [68] deployed the PIV technique to contrast  
598 horizontal and vertical deformations of a model slope, before and after modification with waste carpet  
599 fibres. More recently, [69] assembled a PIV strongbox on a standard beam-centrifuge to visualise flow  
600 and understand its mechanisms as test penetrometers were driven into a sequenced clayey soil (Fig.  
601 12). There is scope for use of this technique in tracing the displacement of fines through the soil pore  
602 network.

603

604 **Fig. 12** Soil flow mechanism as a T-bar penetrates stiff clay and pushes through an underlying soft clay  
605 stratum –  $D_t$  is the bar diameter;  $d$  is its vertical displacement and  $x$  is its horizontal displacement [69].

606

### 607 **3. Advances in Materials**

608 An emerging sub-discipline in geotechnical engineering is bio-geotechnical engineering that includes  
609 two streams of processes; these are bio-mediated processes, where interventions are directly  
610 managed and controlled through biological activities and living organisms; and bio-inspired processes,  
611 where interventions are abiotic, and designed to be inspired by biological principles. The latter is also  
612 often referred to as nature-inspired abiotic processes and involves the use of non-living organisms.  
613 Core objectives of biogeotechnological interventions are, first, to accelerate beneficial organic and  
614 biologic processes to occur in a time frame of interest, and, second, to induce adverse processes in a

615 context where the effect is beneficial [70]. This sub-discipline often appears in literature under Nature-  
 616 Based Solutions (NBSs) that refer to technologies and materials used to preserve and sustainably  
 617 manage the ecosystems, and also to restore ecosystems' degraded functions.

618

### 619 3.1 Bio-mediated Materials

#### 620 3.1.1 Deep-rooted vegetation

621 Use of vegetation for stabilisation of earth structures, including infrastructure and natural slopes, has  
 622 attracted much interest in recent years. The emphasis in the past few years has been on understanding  
 623 the role of vegetation in the context of the slope–vegetation–atmosphere interaction through cutting-  
 624 edge field monitoring and testing. [71] presented a recent important state-of-the-art review on  
 625 impacts of climate change in the context of engineered slopes for infrastructure. The work offers a  
 626 European perspective and is written by members of COST Action TU1202.

627 Other recent pivotal contributions include field survey of desiccation cracking of clay-fill  
 628 embankments, with reference to atmospheric and soil–hydrological specific conditions ([72] – Fig.  
 629 13a). [73] deployed a Fortran95 powered two-dimensional slope stability model with hydrological and  
 630 vegetation effects, SSHV-2D, to incorporate evapotranspiration-induced temporal and spatial  
 631 distribution of water content on the mechanical effects of the vegetation and overall implications on  
 632 slope stability [73]. [74] studied the impact of selected deep-rooted vegetation cover on the  
 633 hydrological balance at the ground surface. [74-76] reported on a 3-year monitoring programme of  
 634 surficial desiccation cracking, piezometric-head fluctuations, soil matric-suction levels and hence  
 635 shear strength as part of a crop test at the toe area of the Pisciola ([74-76] – Fig. 13b). The Pisciola  
 636 landslide was deemed to follow a slow and deep weather-induced mechanism. As such, [74]  
 637 considered the vegetation layer only in terms of hydraulic reinforcement (i.e., evaporation and  
 638 transpiration rates). The team reported on seeding several deep-rooted crop types belonging to two  
 639 vegetation families: the *leguminous*, belonging to the “C3 carbon fixation” type [77-80] (Fig. 13c), and  
 640 the *Gramineae*, belonging to the “C4 carbon fixation” type [81-82] (Fig. 13d). Such crop families differ  
 641 basically in leaf structure and consequently biological activity and in the vegetation life cycle [83]. In  
 642 particular, the C4-cycle crops are generally referred to as evergreen plants, as they exhibit high  
 643 photosynthesis potentials and water retention capacities [84].

644

645 **Fig. 13** (a) BIONICS research embankment, in northern England, covered to the north with grasses  
 646 (e.g., *Alopecurus pratense* and *Lolium perenne*) and to the south with wildflowers (e.g., *Leucanthemum*

647 *vulgare*, *Filipendula ulmaria*, *Achillea millefolium* and *Knautia arvensis*). Instrumentations allow  
 648 measurement of volumetric water content, electrical conductivity and soil temperature [72]; (b)  
 649 Pisciolo hillslope in southern Italy covered with (c) C3-cycle *leguminous* and (d) C4-cycle *Gramineae*  
 650 plants [85]

651

652 The C3-cycle crops are not able to control the stomata closure, such that water is likely to exit the  
 653 plant system in the form of water vapour [83], causing the plant to eventually wilt. With reference to  
 654 the monitoring data of the Pisciolo test site, [74] reported preliminary data of the impact of selected  
 655 deep-rooted vegetation on the soil state at depth. In particular, the vegetation has been seen to act  
 656 as a heat filter, reducing temperature fluctuations in the subsoil, with reference to spontaneous and  
 657 sparse vegetation. [74] reported lower orders of the water content in soil throughout the year up to  
 658 1.6 m depth, as compared to soils covered with spontaneous vegetation. Hydraulic conductivity and  
 659 retention properties of the soil appear to be strongly impacted by the root system of the selected  
 660 vegetation [86-88]. In particular, published preliminary monitoring data suggests a one order of  
 661 magnitude increase in the saturated hydraulic conductivity for the rooted soils, compared to unrooted  
 662 soils. The water retention capacity of rooted soils appears to resemble those of coarser soils. This is  
 663 manifested by the significant lower orders of air-entry value [74].

664

### 665 3.1.2 Biocement

666 By 2016, there were some 2400 publications on 15 types of biocements across a spectrum of  
 667 disciplines, including microbiology, enzymology, biogeochemistry, and mineralogy of biocementations  
 668 [89]. Examples of natural biocementation signatures on earth include sandstones and are brought in  
 669 Fig. 14.

670 Biocements are generally used in the construction industry, where there is a need for a low-  
 671 viscosity cementing solution for filling pores through injection, or to control soil erosion and dust  
 672 deflation through spraying. However, these are generally more expensive than traditional cement,  
 673 costing between 200 and 250 US\$/t. This is above 100 US\$/t, the approximate present maximum cost  
 674 of novel materials for economic viability [89].

675

676 **Fig. 14** Signatures of natural biocementation in sandstone: (a) Bryce Canyon National Park, Utah, USA  
 677 [90]; (b) Arches National Park, Utah, USA [91]; (c) The Belogradchik, Vidin, Bulgaria [92]

678

679 Biocements contain two-to-four components: (1) a main structural component which can include salts  
 680 of  $\text{Ca}^{2+}$ ,  $\text{Ca}^{2+}$  and  $\text{Mg}^{2+}$ , or  $\text{Fe}^{3+}$ ; (2) a pH-controlling component, that can be urea, nitrate, phosphate,  
 681 acetate, or formate; (3) a bio-controlling component, that can be specific microbial cells or enzymes;  
 682 and (4) a biopolymer to form the 3D structure of biocement and improve the overall mechanical  
 683 properties [93]. A limitation common to the vast volume of published works on this topic is little  
 684 insights from expert biotechnologists. Effective design of biocements require inputs from  
 685 biotechnologist with expert knowledge of microbiology and biochemistry, alongside civil/geotechnical  
 686 engineers. One of the most recently developed biocement types is Hydroxyapatite [94], a product of  
 687 bones from meat-processing wastes, that can be used in conjunction with elastic biopolymers to  
 688 diminish brittleness.

689

### 690 3.1.3 Bacterial Biofilm

691 Bacteria rarely grow as unicellular planktonic cultures. Instead, bacteria predominantly exist as  
 692 communities of sessile cells in the form of biofilm [95]. Biofilms (Fig. 15a) are structures comprising  
 693 microorganisms surrounded by a matrix that allows their attachment to inert (e.g., soil particles) and  
 694 organic (e.g., mucosa) surfaces. They are a product of bacterial transition from the unicellular  
 695 (planktonic) life phase to multicellular (sessile cells). Once attached to surface, they multiply and  
 696 begin to produce/exude extracellular polymeric substances (EPS), which assist them to form bacterial  
 697 colonies. Growth of colonies does not last forever; these break up via desorption, detachment or  
 698 dispersion, releasing bacteria and biogenic gas back to the surrounding medium. In the case of soils,  
 699 this medium is the soil pore space. Bacteria may fill pore spaces or form inter-particle bridge and  
 700 buttress connectors, or may clog pore throats, or coat soil particles (soft viscous biofilms) – Fig 15b.  
 701 Bacterial biofilm are soft, viscous, ductile, and elastomeric. They enhance damping and small-strain  
 702 stiffness of soil.

703 Two examples of benefitting from biofilms in sands are presented here.

704 [96] compared the impact of two different microbial biofilms — from multiplication of  
 705 *Shewanella oneidensis* (MR-1) and *Pseudomonas putida* bacteria in a cocktail of Tryptic soy broth,  
 706 sucrose and phosphate buffer — on the behaviour of Ottawa 110 sand. They reported a sharp,  
 707 substantial and rapid decrease in permeability (unwelcomed in the context of NiSE), no change to the  
 708 compression P-wave velocity (measured by piezoceramic transducer) over time, an increase in shear  
 709 S-wave velocity (measured by bender elements), no change to P-wave peak-to-peak amplitude and,  
 710 hence, the pace of seismic waves attenuation. To this end, both biofilms attenuate seismic wave  
 711 propagation at the cost of decrease in permeability. The second important recent contribution is the

712 work of [97] on growing bacterial Dextran in clean sand. They grew an aerobic bacteria, *Leuconostoc*  
 713 *mesenteroides*, in a cocktail of yeast extract, sucrose and phosphate buffer to generate a viscous  
 714 Dextran biopolymer (Fig. 15c), coating sand grains. Dry sand mixed with bacterial culture was  
 715 compacted in layers to reach a compacted void ratio of 0.6, with monitoring of the geophysical  
 716 properties of the mediated sand performed over the following 41-d period. They showed no changes  
 717 to the shear modulus and stiffness over time, a progressive decrease in permeability, welcomed  
 718 decreases in P- and S-wave peak-to-peak amplitudes — indicating a faster attenuation of waves,  
 719 decreased wave propagation, and a medium that better conveys seismic waves.

720

#### 721 3.1.4 Biological Carbonate Precipitation Technologies (CPT)

722 Carbonate precipitation technologies (CPT) began to gain interest from the early 21<sup>st</sup> century, offering  
 723 a spectrum of applications, including solid-phase capture and remediation of problematic trace metals  
 724 and radionuclides [98], remediation of fractures in concrete [99], carbon sequestration [100], and  
 725 improvement of soil and fractured rock. Biological CPT or managed precipitation of calcium carbonate  
 726 through ureolysis fits both bio-inspired and bio-mediated ground remediation techniques and has  
 727 potential to seal porosity and/or to enhance soil steady states at an almost unchanged macro-scale  
 728 void ratio. Ureolysis occurs through the hydrolysis of urea to ammonia ( $\text{NH}_3$ ) and carbonic acid,  
 729 subsequent equilibrium in pore water and formation of bicarbonate, ammonium ( $\text{NH}_4^+$ ), and  
 730 hydroxide ( $\text{OH}^-$ ) ions. The elevated pH from  $\text{OH}^-$  ions and abundance of bicarbonates trigger  
 731 precipitation of calcium carbonate — preferentially calcite polymorph [101]. However, the technique  
 732 is mainly only applicable to fine sand or coarser soils. Recent work by [102] casts doubt on the  
 733 appropriateness of using standard sands (e.g., Ottawa 20-30) for biological CPT-treatment trials and  
 734 geomechanical testing. This shows the importance of full-scale (field) trials that, to date, have largely  
 735 failed to attract much interest — due to costs, quality assurance, quality control, possible  
 736 environmental impacts, and logistical constraints. The implications of the toxic ammonium chloride  
 737 by-product of ureolysis continues to be a concern [103]. To bring this into context, using CPT treatment  
 738 for sealing of a 100 m (L) by 5 m (W) by 2 m (H) dam can pollute about  $4.5 \times 10^6 \text{ m}^3$  of drinking water  
 739 and  $100 \text{ km}^3$  of air [104].

740

741 **Fig. 15** (a): Bacterial life cycle and biofilm formation [95]; (b): possible forms of bacterial growth on  
 742 soil particle surface [105 — with permission from ASCE]; (c): clean Ottawa sand ( $D_{50} = 120 \mu\text{m}$ ) packed  
 743 to a void ratio of 0.6 (left), transformed into Dextran-mediated sand (middle), where particles are  
 744 coated and bridged at the cost of a decrease in porosity, and hence permeability [97]

745

746 **Microbial-induced carbonate precipitation (MICP)**

747 Bacteria are abundant in soil; for instance, in one gram of soil in top 1 m, there are approximately  
 748  $2 \times 10^9$  bacteria, many of which can survive and thrive at deeper depths. Over the last decade, there  
 749 has been increasing attention over what microbial processes can offer to geotechnical engineering  
 750 [106]. MICP is a biomediated process for precipitation of calcium carbonate [101], desirably at particle  
 751 contact points. In MICP, microbes produce the urease enzyme. *Bacillus pasteurii* – also known as  
 752 *Sporosarcina pasteurii*, an alkalophilic bacterium with a highly active urease enzyme – is a microbe  
 753 type commonly used in MICP via bioaugmentation [107]. Important field trials include the stepwise  
 754 approach devised and implemented by [108]. Figure 16a shows the 0.9 m x 1.1 m x 1 m sand box that  
 755 received 3500 litres of bacterial suspension and 0.5 M urea/CaCl<sub>2</sub> reagent solution in 8 intervals and  
 756 over a 50-d period. Scaling up from 1 m<sup>3</sup> to 100 m<sup>3</sup>, Fig. 16b shows an 8.0 m x 5.6 m x 2.5 m container  
 757 filled with saturated, loose poorly-graded medium siliceous sand (average dry unit weight of 15.6  
 758 kN/m<sup>3</sup>) built by [109] for a large-scale trial. A cocktail of highly ureolytic bacteria suspension and  
 759 urea/CaCl<sub>2</sub> reagent solution was injected sequentially, through three 300-mm dia. PVC injection wells  
 760 at 1 m spacing, and pumped towards three extraction wells at 5 m distance over a 16-d period. Moving  
 761 towards full field-scale, [102] treated 1000 m<sup>3</sup> of soil at depths of between 3 and 20 m below ground  
 762 level by injecting 200 m<sup>3</sup> of bacterial suspension and 300 to 600 m<sup>3</sup> of urea/CaCl<sub>2</sub> reagent solution (Fig.  
 763 16c). Commercially, a handful of contractors use the technique as a means of ground improvement  
 764 for subgrades and retaining structures (Fig. 16d). A limitation of MICP, particularly in soils with small  
 765 pore throats, and in the context of NiSE, is the possibility for bacteria to be physically strained in the  
 766 soil media causing porosity reduction due to biomass clogging [110]. This is manifested in the X-ray CT  
 767 scan in Fig. 17, illustrating the spatially resolved maps of the changing porosity throughout and after  
 768 the MICP process [111].

769

770 **Fig. 16** MICP trials in three scales: (a) cubic meter sand box [103] – photograph from [117]; (b) 100  
 771 cubic meter sand box [109]; (c) 1000 cubic meter field-scale mediation [103]; (d) MICP at large scale:  
 772 MICP-treated 400-mm dia. column by Soletanche-Bachy [118]

773

774 **Fig. 17** 3D visualization of the X-ray CT data illustrating the variation in porosity: (a) pre-MICP  
 775 precipitation; (b) post-MICP precipitation; (c-d) service time under acidic conditions in favour of CaCO<sub>3</sub>  
 776 dissolution [111]

777

778 Exploitation and biostimulation of native microbes continue to attract interest across  
 779 ecological, quaternary geology and geomechanics disciplines [112-113]. However, a major limitation



780 to employing native bacterial communities is the need for adding organic nutrients, such as molasses,  
781 to enrich the biomass [101] and the likely environmental consequences, such as eutrophication. A  
782 thorough review of biogeochemical processes in the geotechnical context is given in [114].

783 More recent 'technological development' attempts include the work of [115], who reported  
784 on staged injection of a cocktail of bacterial cell (*S. pasteurii*) and urea/CaCl<sub>2</sub> solutions, using a pressure  
785 head, into two loose medium sands. For about 6% precipitated calcite and through a comparative  
786 experimental campaign, [116] proposed two injection cycles, each with aeration during injections and  
787 24-h solution retention period, with a 6-d drained stage between cycles, and for 0.5 M cementation  
788 solution. In addition to baseline strength enhancement, the MICP technique has also been  
789 investigated as a technology for stabilisation of crustal layers and mitigation of wind-driven erosion.  
790 [117] developed single- and double-MICP spray treat techniques for loose medium silica sand and fine-  
791 to-medium carbonate sands. They considered a 6-d gap period between the first and the second spray  
792 applications and 28 d of curing post spray treatment. Through referring to findings from wind tunnel  
793 experiments, they demonstrated the singly MICP-spray-treated crustal sand layer exhibited no dust  
794 deflation for simulated 20 m/s winds measured at 20 cm above the treated sand layer surface.

795 MICP has recently been used to make sand cube samples (Fig. 24d), seeded with non-engineered  
796 bacteria and receiving nutrients through multiple and controlled directions [119-120]. Findings  
797 reported in [120] show that influencing factors on the cemented form is not restricted to the form of  
798 the cast (and hence topology of the pore spaces in soil – Fig. 24e,f), and also show how the flow of the  
799 nutrient medium can create a diverse range of cementation zones.

800

#### 801 ***Enzyme-induced carbonate precipitation (EICP)***

802 EICP is a bio-inspired process for precipitation of calcium carbonate to achieve rapid increases in soil  
803 peak strength and dilatancy. The urease in EICP is derived from agricultural sources, such as Jack Bean  
804 (*Canavalia ensiformis*) meal [121]. A recent attempt by [122] to create columns of improved sand by  
805 EICP exhibited an improved UCS of 400 to 500 kPa achieved at approx. 0.8 to 1.7% axial strain.

806 Moving up the scale, [123] reported a recent large-scale attempt to build a 0.3-m dia. × 0.9-m  
807 long EICP-mediated sand column inside a sand box sizing 0.6 x 0.6 x 1.2 (L) m. They injected a cocktail  
808 of urea (1.5 M), CaCl<sub>2</sub> (1 M), 9900 U/l urease enzyme, and 4 g/l no-fat milk powder in three shots using  
809 PVC 1.2-m long tube-à-manchette (TAM). For <3% precipitated calcium carbonate within a 0.3-m dia.  
810 cylindrical treatment zone, they reported an achieved UCS of >500 kPa. They estimated the cost of

811 mediation in the range of \$US 60 per cubic meter of sand. An EICP column and needle penetrometer  
812 test performed in between two subsections of treated column is illustrated in Figure 18.

813

814 **Fig. 18** EICP trials at field-scale: soil column in box test set-up with TAM and packer, and needle  
815 penetrometer measurements done on cemented soil section [123 – with permission from ASCE]

816

#### 817 ***Microbial-induced desaturation and precipitation (MIDP)***

818 An undesirable side-effect of using EICP is the consequent toxic ammonium chloride by-product. MIDP  
819 is another emerging bio-mediated technology, where nitrate-reducing bacteria in the soil are  
820 stimulated to produce biogas and biominerals [124]. Nitrate reduction or denitrification is a novel  
821 recent alternative method, where a combination of calcium fatty acids and calcium nitrate are used  
822 in conjunction with indigenous microbes to precipitate calcium carbonate. The MIDP technique offers  
823 a non-hazardous nitrogen gas by-product, and can achieve significant increases in dilatancy, stiffness,  
824 strength and cyclic resistance of host sands [125]. The application of MIDP should be designed to result  
825 in 1–3% CaCO<sub>3</sub> cementation, which requires 25–70 kg/m<sup>3</sup> substrate and application of the cocktail in  
826 3 to 10 flushes.

827

#### 828 ***Microbially Induced Desaturation (MID)***

829 As an alternative desaturation approach, the required substrate to achieve 10–20% desaturation of  
830 N<sub>2</sub> by the MID approach would decrease to 0.7–1.5 kg/m<sup>3</sup> – that is, roughly 40 times less substrate  
831 required than MICP – and benefits in a single flush application. As such, the MID approach is a  
832 significantly cheaper option compared to other biogeochemical options and has relatively benign side  
833 effects. The technique was recently trailed at field-scale on sandy and silty soils in Harborton – that is,  
834 the area of Oregon’s Critical Energy Infrastructure (CEI) hub – and Sunderland, close to the Portland  
835 International Airport, west side of Portland, USA. The main objective of the trial was liquefaction  
836 mitigation and enhancement of seismic resistance of local industrial infrastructures that supply over  
837 90% energy of Oregon State. Nutrients (calcium nitrate, or fertilizer, and calcium acetate, or food  
838 grade, each 10 g per litre of water) were injected to the ground from a central well and extracted from  
839 perimeter wells (Fig. 19a). The denitrification led to the liberation of N<sub>2</sub> and CO<sub>2</sub> gases, which then  
840 desaturated the soil to remove the potential of liquefaction. In Fig. 19b, the decrease in P-wave  
841 velocity ( $V_p$ ) is indicative of successful desaturation. The treatment period took one month, and  
842 monitoring is ongoing for 3 to 5 years, starting from September 2019.

843

844 **Fig. 19** (a-b) MID test setup in Portland, Oregon, USA: injection probe and monitoring installation,  
845 including cross-hole and downhole TREX sensor array measuring excess porewater pressure,  $V_p$  and  
846  $V_s$ , and CTD divers; (c) measuring fluid volume and salinity, and TEROS-12 sensors; (d) measuring  
847 salinity and temperature; (e) P- and S-wave velocity cross-hole measurements [126]

848

#### 849 ***CPT as a means of self-repairing through an autonomous response to damage***

850 Breakage of brittle binding connectors (i.e., bonds) at particle contacts in a porous medium can lead  
851 to soils' structural failure. However, once damage occurs and the soil skeleton relaxes to a new  
852 equilibrium, the grain contacts might be cemented anew through a *self-healing* ground improvement  
853 system that is both responsive and adaptable. Both autogenous (a natural property of the material  
854 concerned) and autonomous (an engineered property) systems are able to respond to stimuli, such as  
855 bond damage or the presence of deleterious substances (e.g., chlorides in concrete), in order to  
856 counteract the problem. Crack formation in concrete has been addressed through self-healing systems  
857 which produce grouts *in-situ* and at the location of damage, both biologically [127] and chemically  
858 [128], and there is the potential for similar techniques to be applied in grouts for ground improvement.  
859 [129] findings demonstrated the concept of self-healing MICP in sand and limestone, where spore-  
860 forming bacteria are able to generate a calcium carbonate grout *in-situ*; as the grout forms, bacterial  
861 spores entombed in the grout remain until damage occurs, whereupon these spores are exposed and  
862 they can germinate, with the resulting cells able to re-heal the damage through further precipitation.

863

#### 864 **3.1.5 Biopolymer-based soil treatment (BPST)**

865 Whilst most grouts or other bonding agents are strong but brittle, and thus susceptible to fracture in  
866 a porous medium, BPST offers a more resilient response to stress concentration. Due to increased  
867 ductility, they are able to respond to loading through deformation, rather than brittle fracture.  
868 Biopolymers (or natural polymers) are naturally exuded by micro- and macro-organisms (bacteria,  
869 plants, etc), and have been shown to affect soil geotechnical behaviour at low levels [130], although  
870 this is dependent on environmental conditions (particularly moisture), and biodegradability may limit  
871 their durability. However, they are self-sustaining under the right conditions. For instance,  
872 biopolymers obtained from inedible parts of cultivated plants have received recent interest as an  
873 environmentally friendly grout for ground improvement. [131] collated the application of many  
874 common biopolymers in geotechnical engineering. These include xanthan gum (XG) and sodium  
875 alginate (SA) [123], guar gum (GG), and mixtures of agar (from red algae) and enzymatically modified

876 starch [132]. Biopolymers are mostly applied to sands, silts and silty sands in less than 2 wt.% [of soil]  
 877 proportion, and mainly to control the hydraulic conductivity, and also to increase shear strength and  
 878 stiffness. [133] recently reported on the use of a range of biopolymers for improving Shanghai clay  
 879 under repeated traffic loading. This is an interesting contribution given the broad range of biopolymers  
 880 applied to the clay, and it is the first reporting on growth of fungal genus in biopolymer (particularly  
 881 with casein and carrageenan) treated clays. They reported on the use of carrageenan kappa gum (KG),  
 882 locust bean gum (LBG), XG, agar gum, GG, SA, chitosan (CH) and gellan gum (GE).

883 The long-chain structure of biopolymers and certain constituting chemicals (e.g., hydroxyl,  
 884 ester or amines) supply adhesive forces that help coating and binding of soil particles together [132].  
 885 An advantage of BPST over MICP is a better chance of quality/quantity control and the rapid treatment  
 886 process [131]. Biopolymers are produced from exo-cultivating facilities (Fig. 20), requiring relatively  
 887 less time and resources (e.g., nutrients, aeration, cultivation environment control). A possible  
 888 drawback of applying biopolymers on soils, in the context of NiSE, is the consequent elevated  
 889 temperature, change in soil solution pH, and occupation of the void space [134]. Drivability of  
 890 biopolymers in soil has remained a practical drawback. To control 'setting time', [135] applied a broad  
 891 suite of biopolymers to superfine GGBS cement and explored ways to increase the zeta potential of  
 892 fine grout particles for these solids to remain in suspension for reasonable periods of time in order to  
 893 allow implementation of the grouting processes.

894

895 **Fig. 20** Comparison between MICP and BPST processes [124]. Note, in Fig. 20c rods represent soil  
 896 particles and red-coloured lines represent biopolymer chains, with adhesive force among themselves  
 897 and cohesive force between them and the soil particles

898

### 899 3.1.6 Deep-rooted vegetation in biopolymer treated clays

900 A limitation of the deep-rooted vegetation remedial technique is the time required for the growth of  
 901 plants, and hence for the benefits of the technique to materialise. Injection of a viscous solution of  
 902 biopolymers can improve the soil strength at the initial state of plant growth, and meanwhile provides  
 903 carbon, nitrogen and other nutrients needed for plant growth [136].

904

### 905 3.1.7 Fungal mycelial networks

906 Slipping surfaces/zones in earth slopes tends to develop below the rooting zone, and failure is often  
 907 triggered by infiltrating rainwater raising the porewater pressure, thereby reducing the effective

908 stresses and degrading the geomechanical properties. Use of deep-rooted vegetation to remove  
 909 porewater and increase the matric suction, with effects extending below the rooting zone, is fairly  
 910 well established [137] and was discussed earlier in the paper. Alternatively, infiltration may be  
 911 minimized via hydrophobic fungal-hyphal networks [138], or rhizosphere-promoted lateral flow [139].

912 Fungi account for up to 75% of total microbial biomass in soil. Multi-cellular fungi grow in the  
 913 form of hyphae, forming a complex network known as mycelium. Hyphae are typically 1–3  $\mu\text{m}$  in dia.,  
 914 can have lengths from several micron to several metres (Fig. 21a), and they branch out to form  
 915 complex networks. Mycelia networks are massive, incredibly resilient, adaptable and they have an  
 916 ability to recover in the face of damage. In soil science, it is widely acknowledged that fungi contribute  
 917 to soil aggregation and can form soil crusts.

918 A recent interesting contribution in this field is the work of [138], who reported the first case  
 919 of water-repellent sand (Fig. 21d) created using fungal treatment. They treated sterile sands by  
 920 growing *Pleurotus ostreatus* (strain M 2191; i.e., edible oyster mushroom) – with and without source  
 921 of carbon (wood fibres). [140] tested a well-graded sand column of 30-cm high, contained in a Perspex  
 922 cylinder and with a constant head of water on top, to study the impact of fungi growth on ponded  
 923 infiltration (Fig. 21b-c). The fungal mycelium appeared in the form of a visible, dense network of white  
 924 tubular elements that prevented water ingress, forcing the water to convey via preferential flow  
 925 paths. Use of fungi in ground engineering is a new avenue of research within bio-geotechnics and  
 926 offers creation of a hydrophobic surface layer on erodible sands, reduces infiltration, reduces  
 927 saturated hydraulic conductivity, and improves the erosion resistance.

928

929 **Fig. 21** Influence of fungal mycelial networks on soil behaviour: (a) growth of *Pleurotus ostreatus*  
 930 edible fungi in soil; (b-c) growth of fungi in a column of sand; (d) water repellency [140]

931

### 932 **3.2. Bio-inspired Materials**

#### 933 **3.2.1 Imitating organic fibrous matters**

934 Natural fibrous matters in soil include certain calcium carbonate polymorphs (e.g., aragonite),  
 935 reprecipitated carbonates into secondary  $\text{Ca}^{2+}$  minerals near plant root structures, organic fibrous  
 936 matters (e.g., fibrous peats), plant rootlets, rhizolithic calcretes [141], and products of carbon  
 937 sequestration into calcium silicate, dicalcium silicate, tricalcium silicate, tricalcium aluminate and  
 938 similar hydrated products in urban soils [7].

939 Fibre-reinforced soil refers to a soil mass mixed with randomly distributed, short, intertwining  
940 fibres that imitate organic fibrous matters in form. Fibres are added to soil as standalone matters, or  
941 in combination with traditional binders like cement [142].

#### 942 **Opportunities and Challenges**

943 Mixing short fibres with soil is an established ground improvement method for dilative materials  
944 (usually granular soils) and is not conventionally considered effective for clays with a low apparent  
945 friction angle. However, due to the ease of application and reduced environmental impact, the use of  
946 discrete fibres in cohesive soils is gaining interest [143-145]. Effectiveness of fibres is a function of  
947 confining pressure. Fibres may compromise strength of sands and clays at confining pressures greater  
948 than a critical threshold [146-147]. Contribution of fibres is more pronounced for lower confinement  
949 levels and, therefore, indicative of the effectiveness of the technique in shallow ground [147]. Fibre  
950 effectiveness is maximum when soil is subjected to extension and torsion [65]. Fibre surface roughness  
951 play a pivotal role in the mechanical performance of fibre mixed soils [148-149]. Treatment of fibre  
952 surfaces ahead of soil mixing was reported in [150]. A major technical concern in the use of fibres is  
953 the implications of their typical high volume to weight ratio which often disrupts the uniformity of  
954 soil–fibre mixtures; that is, high fibre contents may lead to formation of fibre balls and lumps in the  
955 treated soil. Furthermore, high moisture contents may lead to fibre floating and heterogeneous soil–  
956 fibre mixtures. Distribution and orientation of fibres in soil during service life remain a matter of  
957 debate [65-66].

958 Overall, fibres in soil provide enhanced levels of shear strength [151], decrease residual  
959 strength loss [152], mobilise larger strains at failure, increase strain-hardening and reduce  
960 deformability, lower shrinkage, and relax implications of soil inherent anisotropy and swelling  
961 potential. In laboratory settings, cylindrical test specimens of fibre-reinforced composites typically fail  
962 through bulging, rather than shearing along an inclined plane of weakness, indicative of general ductile  
963 behaviour.

964 When introduced to sand, fibres benefit from the ‘rigid wall effect’ to preserve the original  
965 open micro- and macro-pore network. This is, however, a function of fines content in the soil [35]. A  
966 major concern with fibre-reinforced loose sands is the impact of the difference between stiffness of  
967 fibres and mineral solids, and therefore varied interparticle interactions. Figure 22a-b illustrates the  
968 first and second stress–strain hysteresis loops for two sands, A and B. In these figures, the dark bold  
969 curve refers to clean sand, the grey curve refers to sand with little silt content (known as *Small Silt*),  
970 and the light grey curve refers to sand with little silt and 1% fibre. Sand B is relatively coarser, develops  
971 larger strains, and a less abrupt, smoother pathway to the flow failure. This is fundamentally due to

972 the better interlocking between particles. Fibres provide similar service and that raises a key question:  
 973 i.e., how does the varied stiffness between fibres and solids impact on the packing state and overall  
 974 behaviour. Figure 22c-d shows how the dilative behaviour of sand changes to contractive strain-  
 975 softening for the major principal stress axis reorientated to 60° from its initial vertical direction,  
 976 whereas fibres preserve the dilative response, irrespective of principle stress orientation. However,  
 977 fibres fail to fully perform under compressive–torsional stress environments.

978 When introduced to clays, fibres are reported to compromise dilation and promote build-up  
 979 of excess pore-water pressure under undrained shearing conditions [153]. Failure along distinct slip  
 980 planes within unreinforced clays changes to a barrelling type of failure in fibre-reinforced soils. For  
 981 clays, typical content of synthetic fibres is 0.2 to 1 wt.%, while for recycled waste fibres, this ratio is  
 982 higher at between 1 and 5 wt.%.

983

984 **Fig. 22** Consolidated-undrained (CU) behaviour of sands and fibre-reinforced sands under cyclic and  
 985 anisotropic loading conditions (a and b): first and second stress–strain hysteresis loops for two sands,  
 986 mixed with silt and fibre [35]; (c): HCTS CU results for sand, with and without fibre reinforcement,  
 987 showing stress–strain curves for  $p' = 400$  kPa,  $\alpha = 30^\circ$ , and  $b = 0.5$  and  $1.0$  (compression and torsion)  
 988 [65]; (d) HCTS results for sand, with and without fibre reinforcement showing stress–strain curves for  
 989  $p' = 400$  kPa,  $\alpha = 60^\circ$ ,  $b = 0.5$  and  $1.0$  (torsion). Note: HCTS, hollow cylinder torsional shear;  $p'$ , effective  
 990 mean normal stress;  $\alpha$ , principal stress orientation to vertical direction;  $b$ , intermediate principal stress  
 991 ratio [65]

992

### 993 **Fibre typology**

994 Figure 23 presents snapshots of a range of common natural and synthetic fibre types employed in  
 995 ground engineering. These include natural fibres of wool, jute [154], coir [67], sisal, palm, and flax,  
 996 and synthetic fibres of polypropylene [143], nylon, fibreglass, rubber, polyvinyl alcohol [155],  
 997 polyethylene and polyamide. Common recycled fibres used in ground improvement are a range of  
 998 scrap tyre materials spanning across the particle-size range spectrum, including granulated tyre (sizing  
 999 from 425  $\mu\text{m}$  to 12 mm), tyre chips (sizing from 12 to 50 mm), and tyre shreds (sizing from 50 to 305  
 1000 mm) [32].

1001 Employment of unconventional upcycled fibres has attracted some recent interest, including  
 1002 shred waste-carpet fibres [156], and precipitated calcium carbonate (PCC) obtained from sucrose  
 1003 ( $\text{C}_{12}\text{H}_{22}\text{O}_{11}$ ) juice purification during sugar production [157].

1004

1005 **Fig. 23** Examples of natural, synthetic and recycled fibres sometimes mixed in soil to imitate plant  
 1006 rootlet reinforcement effect: (a) coir [158]; (b) nylon – virgin synthetic [158]; (c) polypropylene – virgin  
 1007 synthetic [158]; (d) fibreglass – virgin synthetic [158]; (e-f) waste carpet [156]; (g) jute [154 – with  
 1008 permission from ASCE]; (h): coir [67]; (i) thermoplastic polymeric microsynthetic [65]; (j) granulated  
 1009 tyre [159]

1010

### 1011 3.2.2 Imitating weathered minerals

1012 [160] attributed the origin of amorphous silica in soil to chemical and thermal weathering and series  
 1013 of dissolution–reprecipitation processes. Amorphous silica in soil can appear in the form of a smooth  
 1014 ‘onionskin’ shield around quartz particles, or individual rounded flocs that occupy soil pore spaces  
 1015 [161]. The coating and filling functions of these fine weathered minerals in soil have led to a surge in  
 1016 development of a range of nanomaterials, including nano-silica (NS) and nano-clay (NC). Recent  
 1017 contributions include the use of colloidal NS hydrosols in reconstruction of naturally porous loessic  
 1018 brickearths [25], and to mediate a range of soils, including dune sands [162] and peat [163].

1019 Weathering of minerals can lead to geochemical changes in soil, triggering a range of reactions  
 1020 that can generate novel binders. A simple form of such reactions is deprotonation of clays in alkaline  
 1021 environments, and formation of C-S-H gels in the presence of calcium source. The binding matrix can  
 1022 be imitated to synthesise complex geopolymers. Geopolymerisation refers to thermal and chemical  
 1023 interactions between aluminosilicate-rich materials (e.g., clay, fly ash (FA), slag) and alkaline solutions  
 1024 (e.g., NaOH, Na<sub>2</sub>SiO<sub>3</sub>) for formation of inorganic polymers of alumina and silica. The process resembles  
 1025 hydration of Portland cement, but leaves behind little carbon footprint. Using geopolymerisation for  
 1026 stabilisation of domestic solid wastes has gained some recent interest; for instance, [164] deployed  
 1027 geopolymerisation to stabilise spent ground coffee (collected from coffee brewing cafes) into road  
 1028 subgrades. Other novel forms of geopolymers used in ground engineering include FA and slag-based  
 1029 geopolymers [165], FA–calcium-carbide residue CCR (by-product of acetylene gas production) based  
 1030 geopolymers [166], recycled asphalt pavement (RAP) and FA geopolymer [167], as well as eggshell  
 1031 powder (from crushing waste eggshells) and FA (from coal-fired electricity production plant) [168].

### 1032 3.2.3 Engineered biological matters (synthetic biology)

1033 Bone is an adaptive living material. When loaded repeatedly, bone responds to the stimulus and cells  
 1034 grow to make the system stronger. There is interest to engineer simple organisms to have this type of  
 1035 responsive behaviour (i.e., different from how they behave in nature). This idea was the philosophy  
 1036 behind the recent Newcastle University and University of Northumbria ‘Thinking Soils’ project, which  
 1037 aims to develop a material containing engineered bacteria that strengthens itself in respond to load.  
 1038 The project concept [169] was to create a volume of soil (Fig. 24a) that is saturated with water, all the



1039 nutrients that bacteria need present, along with bacterium *E. Coli.* that are engineered [119] to  
1040 respond to pressure. When load is applied, the porewater pressure in the soil volume rises, and the  
1041 bacteria respond to that pressure by initiating a process of calcium carbonate cementation. As the  
1042 load is maintained, pressure is maintained, and the soil becomes strengthened in response. At the  
1043 laboratory scale, genetically engineered bacteria are grown in agar-based hydrogels (see Fig. 24c for  
1044 microstructure), which have some similar mechanical properties to clays [170]. In these experiments,  
1045 the hydrogel acts as a soil analogue, which allows good visualisation of the bacteria and control over  
1046 culturing and growth in 3D.

1047 Imitation of bones may also attract the interest of the permafrost research. Permafrost is a  
1048 complex multiphase porous material, comprised of ice lenses, pore ice, unfrozen water and air.  
1049 Characterisation of permafrost as a porous medium depends on the amount of ice and unfrozen water  
1050 in the pores, which is nearly impossible to determine through common intrusive and non-intrusive  
1051 geophysical techniques. Recently, [172] reported on transient acoustic waves propagating in a  
1052 cancellous bone-like material and the use of theory of poroelasticity to study the effects of porosity  
1053 and pore fluid on the stress distribution, deformation, and reflected and transmitted pressures of the  
1054 bone-like material. The idea was extrapolated in [173-174] for non-destructive determination of bulk  
1055 modulus, shear modulus, porosity, unfrozen water content and ice content of permafrost material.

1056

## 1057 **5. Closing Remarks**

1058 It is intuitively established that the geomechanical behaviour of natural soils varies within, and  
1059 depends on their frame elements, bonding elements, voids that accommodate air, water and  
1060 microorganisms, and importantly the form and structure that relates these to one another. As such,  
1061 natural soil behaviour encompasses a wealth of chemo-bio-physical processes. Frame elements vary  
1062 in size, sorting, shape, texture, and crystalline properties. In natural form, elements and systems that  
1063 make up natural soils are self-healing, self-producing, and self-forming. They constantly evolve, adopt  
1064 form and roles in response to environment, and re-establish functions that are disrupted in the natural  
1065 erosive and stress environment. These *properties*, collectively, mark the fundamental difference  
1066 between natural and engineered ground, as two different types of grand systems. Engineered ground  
1067 is a product of mechanical and/or chemical densification, with a sole mission of enhancing stiffness,  
1068 and stress at steady states, at the cost of filling and compacting void spaces, and replacing air, water  
1069 and microorganisms therein with calcium-based cements, and alike. This transforms the natural  
1070 ground into a self-standing (e.g., for cuttings), impermeable (to control groundwater or line buried  
1071 solid wastes), strong and stiff (to bear superstructure loads) medium. This also disrupts the

1072 biogeochemical cycles and self-forming, self-healing capacities of forms and structures, which are  
 1073 reliant on the soils' intertwining pore network, and driven by interaction amongst frame and bonding  
 1074 elements, and also the living organisms.

1075 To this end, and in the context of NiSE, the next generation of engineering interventions  
 1076 should achieve the following objectives: (1) eliminate the need for exogenous contact-point  
 1077 reinforcement by manipulating soil grain surface properties; (2) employ alternative bonding agents  
 1078 that offer greater toughness and ductility than traditional (brittle) materials; (3) form a porous  
 1079 cemented system that accepts bond breaking as an inevitability, but which is capable of adapting and  
 1080 self-repairing through an autonomous response to damage. In this, engineered ground in the context  
 1081 of NiSE is more sustainable (allowed to continue having functions well beyond a source of heat, water,  
 1082 minerals, and stiff foundation), resilient (arranged to continue functioning in the face of extreme  
 1083 climates), self-forming (designed to be reliant on interactions among self-producing, self-healing  
 1084 evolving components), and adaptable, all contributing to enhanced societal wellbeing (refer to Fig.  
 1085 1a). Through re-establishing the balance between engineered and natural systems in ground, and also  
 1086 restoration of degraded ground function in line with the NiSE concept of appropriating the methods,  
 1087 materials and models according to the above objectives, this paper presented various examples to  
 1088 illustrate how the ground engineering is being rethought, and how ground is being rebalanced with  
 1089 natural systems.

1090

1091 **Fig. 24** Sculpting soil responses to force by altering sequences of DNA and through the interaction of  
 1092 many different genetic devices and engineered organisms: (a) artists impression of a bio-based self-  
 1093 constructing foundation [170]; (b) unconfined compression performed on a column of agarose gel  
 1094 [171]; (c) microstructure of Agarose LM gel [170]; (d) simulation of multilateral flow (growth media  
 1095 for bacteria) and implications of 3D architecture of cementation in sands [120]; (e-f) 3D sand forms,  
 1096 scanned as excavation takes place, in seeking an insight into cementation process [120]

1097

## 1098 6. Conclusions

1099 The ideal engineered ground within the NiSE framework is a complex ground system, in that  
 1100 its constituting geologic and biogenic elements and systems are adaptive, responsive, self-healing,  
 1101 self-producing, self-forming, fractal and intertwined. Instated within is at least one of four basic types  
 1102 of imitable traits abstracted from nature: i.e., forms, materials, generative processes and functions.

1103 Key findings drawn from this contribution are:

1104 1. NiSE is translated into an adaptability indicator system. This is a simple vetting tool,  
 1105 illustrated in Fig. 1b, for bio-inspired/mimetic materials used in ground engineering. Materials receive

1106 a five-scoring scale in three categories of forms, functions and processes. Methods and models enable  
1107 materials to be instated in ground.

1108 2. Models, in the NiSE context, drupe a spectrum of scales, from nano- to meso- to micro.

1109 - Nanoscale models avail studying atomistic-level interactions between biomimetic  
1110 substances and soil particles. These include dissolution, precipitation, nucleation, evolution, ageing,  
1111 and degradation in a thermodynamics and kinetics context.

1112 - Mesoscale models give insight into rate and mechanisms of nanoparticle agglomeration and  
1113 self-organisation of minerals and biogenic substances. Techniques lag behind in simulating long  
1114 timescale processes (e.g., fatigue and hydration) in small length scales.

1115 - Microscale models, particularly those based on the Discrete Element Method (DEM) allow  
1116 an abstraction of reality by treating individual particles as discontinuous elements that interact  
1117 through rheological contact laws. Findings directly feed into constitutive models and design. When  
1118 paired with spectroscopic methods (e.g., coupled LSDEM and  $\mu$ CT), the combined technology allows  
1119 accurate determination of contact force distribution among particles of measured morphology.

1120 - Engineered soils, in the NiSE context, demand bespoke or adjusted constitutive models.  
1121 There is scope for further development of mesoscale models to incorporate complex long-timescale  
1122 processes, like fragmentation and particle breakage, and ways the bio-inspired/mediated materials  
1123 intervene, into future constitutive models. Coupled microscale models with imaging techniques can  
1124 similarly be of benefit. A recent technological solution is making combined use of DEM (an established  
1125 microscale technique), in-situ synchrotron radiography, and thermographic imaging.

1126 - Engineering structured and fissured fine soils, particularly when mixed with bio-inspired  
1127 fibrous matters, could largely benefit from advances in microscale models as standalone, or in  
1128 conjunction with imaging techniques (particularly CT).

1129 3. Methods for visualisation of particle-level events have seen substantial recent advances.

1130 -  $\mu$ CT inform micro-scale models through visualising the size, shape, topology, and evolution  
1131 of pore throats, interacting rigid and soft particles, and fines movement through pore networks. The  
1132 technique provides real-time images of soil pore spaces in evolution, also evolving orientation and  
1133 tortuosity of fibrous matters in soil

1134 - PIV uses consecutive imaging of individual particles in movement within a particulate media.  
1135 There is scope for wider use of PIV in studying the inherent and induced anisotropy in engineered  
1136 soils.

1137 4. Advances and new avenues of research on bio-mediated materials are summarised here;

1138 - Deep rooted C3- and C4-cycle crops benefit in relaxing and curbing temperature fluctuations  
1139 in the subsoil. Key gains are enhanced levels of saturated hydraulic conductivity, lowered air-entry  
1140 value and adjusted water retention capacity to levels typical for coarser soils. A key obstacle, however,  
1141 is the time required for the growth of plants. When used in conjunction with viscose biopolymer  
1142 solutions, mechanical benefits materialise from the outset, and growth of rootlets gain momentum in  
1143 the presence of excess carbon, nitrogen and nutrients.

1144 - Over 15 types of biocements, with varying constituting salt structure, biopolymer, pH-  
1145 controlling and bio-controlling components, are established with scopes as pore void infill or soil  
1146 biocrust; yet, the cost revolves typically around 2 to 2.5-times greater compared to that for Portland  
1147 cement.

1148 - Bacterial biofilms, products of bacteria multiplication on surfaces, form as soft, viscous,  
1149 ductile and elastomeric binders in soil pores, in between and around soil particles, and pore throats.  
1150 They benefit in enhanced damping and small-strain stiffness, but risk modest decrease in permeability  
1151 and a potential of resonance under high-frequency cyclic loads. Research is tending towards  
1152 development of biofilms that offer a decrease in P- and S-wave peak-to-peak amplitudes and faster  
1153 wave attenuation.

1154 - Biological CPT, via ureolysis and EICP (where enzymes are from agricultural sources), can  
1155 benefit in a number of ways, including strength improvement of sands, capture of trace metals and  
1156 radionuclides, at a cost of modest decrease in void ratio. However, large-scale trials have largely failed  
1157 to attract interest due to cost, logistical constraints, and possible implications of toxic ammonium  
1158 chloride from ureolysis.

1159 - MIDP is an emerging safer and cheaper alternative to CPT and EICP. The technique involves  
1160 stimulation of indigenous microbes to produce non-hazardous biogas and biominerals.

1161 - Microbial CPT (MICP) is relatively better established and enjoys a body of published articles  
1162 on full scale (field) testing. Loss of permeability through biomass clogging continues to be a concern.

1163 - Biostimulation of native microbes, as an MICP technique, is receiving increasing interest.  
1164 Eutrophication remains an environmental constraint, as the technique requires biomass enriching  
1165 through addition of organic nutrients, such as molasses.

1166 - Biopolymers offer better ductility, lower cost, rapid treatment, and an opportunity for quality  
 1167 control post-application. However, their application to ground may lead to heating, change in soil pH,  
 1168 and pore clogging.

1169 5. Advances and new avenues of research on bio-inspired materials are summarised here;

1170 - Future research on the development of genetically engineered bacteria that exhibit  
 1171 pressure-responsive behaviour shows promise; as does the use of bacterial spores entombed in grouts  
 1172 that germinate upon exposure to air, thereby assisting damaged binders to self-heal; and the  
 1173 utilisation of fungal networks to create water-repellent hydrophobic surfaces as a means for erosion  
 1174 control.

1175 - Future sees research into unconventional, upcycled fibres types, and ways for their  
 1176 appropriate and optimum uses in strengthening soils with high fines content.

1177 - Recent attempts in imitation of natural weathering of minerals has led to a surge in  
 1178 development of NS, NC, and inorganic geopolymers of alumina and silica, with very little carbon  
 1179 footprint. This is a novel branch of research, with emphasis on geopolymerisation, that allows the use  
 1180 of unconventional wastes (e.g., sugar refinery wastes, spent ground coffee, and eggshell) in ground  
 1181 improvement.

1182

### 1183 Acknowledgements

1184 This contribution partly reports the outcomes of the first NiSE Workshop (NiSE1) that took place online  
 1185 from London, UK, 11–12th February 2021. The workshop organisers thank Prof Catherine O’Sullivan  
 1186 and Prof Hassan Abdalla for opening the sessions. They also thank Prof Volodymyr Ivanov, Dr Victor  
 1187 Stabnikov, Dr Gil H. Ochoa-Gonzalez, Dr Jose Manuel Ramirez Leon, Prof Liz Varga, Prof Darryl  
 1188 Newport, Dr Bamdad Ayati, Dr Bilal Kaddouh, Dr Mehran Eskandari Torbaghan, Dr Munsamy Logan,  
 1189 Dr Sohrab Donyavi, Dr Aryan Hojjati, and Dr Ching Hung for their contributions to the workshop.

### 1190 References

- 1191 [1] Assadi-Langroudi A, Jefferson I, O'Hara-Dhand K, Smalley I (2014) Micromechanics of quartz sand  
 1192 breakage in a fractal context. *Geomorphology*, 211:1-10
- 1193 [2] Assadi Langroudi A, Theron E (2019) Gaps in particulate matters: Formation, mechanisms,  
 1194 implications. In Jacobsz SW (Ed) *Proceedings of the 17th African Regional Conference on Soil*

Formatted: Font: (Default) +Body (Calibri), 11 pt

**Deleted:** This contribution partly reports the outcomes of the first NiSE Workshop (NiSE1) that took place online (hosted from London, UK) 11–12<sup>th</sup> February 2021. The workshop organisers thank Prof Catherine O’Sullivan and Prof Hassan Abdalla for opening the sessions. They also thank Prof Volodymyr Ivanov, Dr Victor Stabnikov, Dr Gil H. Ochoa Gonzalez, Dr Jose Manuel Ramirez Leon, Prof Liz Varga, Prof Darryl Newport, Dr Bamdad Ayati, Dr Bilal Kaddouh, Dr Mehran Eskandari Torbaghan, Dr Munsamy Logan, Dr Sohrab Donyavi, and Dr Aryan Hojjati for their contributions to the workshop.¶

- 1206 Mechanics and Geotechnical Engineering, International Society for Soil Mechanics and Geotechnical  
1207 Engineering, pp 169-179.
- 1208 [3] ISO 18458 (2015) Biomimetics – Terminology, concepts and methodology. International  
1209 Organization for Standards, Geneva, Switzerland.
- 1210 [4] Vincent JFV (2009) Biomimetics - A review. Proceedings of the Institution of Mechanical Engineers,  
1211 Part H: Journal of Engineering in Medicine, 223(8):919-939.
- 1212 [5] Gruber P, Bruckner D, Hellmich C, Schmiedmayer HB, Stachelberger H, Gebeshuber IC  
1213 (2011) Biomimetics - Materials, Structures and Processes: Examples, Ideas and Case Studies. Springer-  
1214 Verlag Berlin Heidelberg.
- 1215 [6] Aristotle (2008) Aristotle Physics. In Bostock D (Ed), Waterfield R (Translator). OUP Oxford, pp 38-  
1216 41
- 1217 [7] Assadi-Langroudi A, Theron E, Ghadr S (2021) Sequestration of carbon in pedogenic carbonates  
1218 and silicates from construction and demolition wastes. Construction and Building Materials, 286:  
1219 122658
- 1220 [8] Masoero E (2021) Simulating the chemo-mechanical behaviour of minerals at the nano-to-micro  
1221 mesoscale, In First NiSE Workshop (NiSE1), 11-12 February, University of East London, London, UK.
- 1222 [9] Ebrahimi D, Pellenq RJM, Whittle AJ (2016) Mesoscale simulation of clay aggregate formation and  
1223 mechanical properties. Granular Matter, 18(3):1-8.
- 1224 [10] Bandera S, O'Sullivan C, Angioletti-Uberti S, Tangney P (2019) An evaluation of contact models for  
1225 particle-scale simulation of clay. E3S Web of Conferences, EDP Sciences, 92:14001.
- 1226 [11] Hanley KJ, O'Sullivan C, Byrne EP, Cronin K (2012) Discrete element modelling of the quasi-static  
1227 uniaxial compression of individual infant formula agglomerates. Particuology, 10(5):523-531.
- 1228 [12] Su TC, O'Sullivan C, Nagira T, Yasuda H, Gourlay CM (2019) Semi-solid deformation of Al-Cu alloys:  
1229 A quantitative comparison between real-time imaging and coupled LBM-DEM simulations. Acta  
1230 Materialia, 163:208-225.
- 1231 [13] Altuhafi FN, O'Sullivan C, Sammonds P, Su TC, Gourlay CM (2021) Triaxial compression on semi-  
1232 solid alloys. Metallurgical and Materials Transactions A, 52(5):2010-2023.
- 1233 [14] O'Sullivan C (2021) How can fundamental modelling and observation inform NiSE? In First NiSE  
1234 Workshop (NiSE1), 11-12 February, University of East London, London, UK.

- 1235 [15] Mesinc (2021) Metrics engineering supply chains. <https://www.mesinc.net/>. Accessed 09 July  
1236 2021.
- 1237 [16] Fathalikhani M, Graham J, Kurz D, Maghoul P (In Press) Investigation and modification of a CSSM-  
1238 based elastic–thermoviscoplastic model for clay, *International Journal of Geomechanics (ASCE)*.
- 1239 [17] Safavizadeh S, Montoya BM, Gabr MA (2019) Microbial induced calcium carbonate precipitation  
1240 in coal ash. *Géotechnique*, 69(8): 727-740.
- 1241 [18] Hall SA, Bornert M, Desrues J, Pannier Y, Lenoir N, Viggiani G, Bésuelle P (2010) Discrete and  
1242 continuum analysis of localised deformation in sand using X-ray  $\mu$ CT and volumetric digital image  
1243 correlation. *Géotechnique*, 60(5): 315-322.
- 1244 [19] Andò E, Hall SA, Viggiani G, Desrues J, Bésuelle P (2012a) Experimental micromechanics: Grain-  
1245 scale observation of sand deformation. *Géotechnique Letters*, 2(3):107-112.
- 1246 [20] Andò E, Hall SA, Viggiani G, Desrues J, Bésuelle P (2012b) Grain-scale experimental investigation  
1247 of localised deformation in sand: A discrete particle tracking approach. *Acta Geotechnica* 7(1):1-13.
- 1248 [21] Cygan RT, Kubicki JD (2001) Molecular modeling theory: Applications in the geosciences, De  
1249 Gruyter, <https://doi.org/10.1515/9781501508721>.
- 1250 [22] Duque Redondo E (2018) Atomistic simulations of confined species in 2D nanostructures: clays  
1251 and CSH gel. PhD Dissertation, University of the Basque Country, Spain.
- 1252 [23] Buchy HN, Katti KS, Katti DR (2020) Modeling the behavior of organic kerogen in the proximity of  
1253 calcite mineral by molecular dynamics simulations, *Energy and Fuels*, 34(3):2849-2860.
- 1254 [24] Gu W, Li X, Li Q, Hou Y, Zheng M, Li Y (2021) Combined remediation of polychlorinated  
1255 naphthalene-contaminated soil under multiple scenarios: An integrated method of genetic  
1256 engineering and environmental remediation technology. *Journal of Hazardous Materials*, 405:  
1257 124139.
- 1258 [25] Assadi-Langroudi A (2014) Micromechanics of Collapse in Loess. PhD Dissertation, University of  
1259 the Birmingham, England, UK.
- 1260 [26] Bauchy M, Masoero E, Ulm FJ, Pellenq R (2015) Creep of bulk CSH: insights from molecular  
1261 dynamics simulations. *CONCREEP* 10:511-516.
- 1262 [27] Shvab I, Brochard L, Manzano H, Masoero E (2017) Precipitation mechanisms of mesoporous  
1263 nanoparticle aggregates: off-lattice, coarse-grained, kinetic simulations. *Crystal Growth and*  
1264 *Design*, 17(3):1316-1327.

- 1265 [28] Ofiteru ID, Masoero E, Taniguchi D, Gebhard S, Mihai I, Jefferson T, Paine K (2020) Engineering  
1266 microbial-induced carbonate precipitation via meso-scale simulations. ASCE Engineering Mechanics  
1267 Institute International Conference, Durham University, Durham, England, UK.
- 1268 [29] Coopamootoo K, Masoero E (2020) Simulations of crystal dissolution using interacting particles:  
1269 Prediction of stress evolution and rates at defects and application to tricalcium silicate. Journal of  
1270 Physical Chemistry C, 124(36):19603-19615.
- 1271 [30] O'Sullivan, C. (2011) Particulate discrete element modelling: a geomechanics perspective. CRC  
1272 Press.
- 1273 [31] Assadi-Langroudi A, Jefferson I (2013) Collapsibility in calcareous clayey loess: A factor of stress-  
1274 hydraulic history. Int J Geomate Geotech Constr Mater Environ, 5(1):620-626
- 1275 [32] Ghadr S, Samadzadeh A, Bahadori H, O'Kelly BC, Assadi-Langroudi A (2021) Liquefaction  
1276 resistance of silty sand with ground rubber additive. International Journal of  
1277 Geomechanics, 21(6):04021076. [https://doi.org/10.1061/\(ASCE\)GM.1943-5622.0002002](https://doi.org/10.1061/(ASCE)GM.1943-5622.0002002)
- 1278 [33] Assadi-Langroudi A, Jefferson I (2016) The response of reworked aerosols to climate through  
1279 estimation of inter-particle forces. International Journal of Environmental Science and  
1280 Technology, 13(4):1159-1168.
- 1281 [34] McDougall J, Kelly D, Barreto D (2013) Particle loss and volume change on dissolution:  
1282 Experimental results and analysis of particle size and amount effects. Acta Geotech, 8:619–62.
- 1283 [35] Ghadr S, Samadzadeh A, Bahadori H, Assadi-Langroudi A (2020) Liquefaction resistance of fibre-  
1284 reinforced silty sands under cyclic loading. Geotextiles and Geomembranes, 48(6):812-827
- 1285 [36] Shire T, O'Sullivan C, Taylor H, Sim WW (2014) Measurement of constriction size distributions  
1286 using three grain-scale methods. Proceedings of the 8th International Conference on Scour and  
1287 Erosion, Oxford, UK, CRC Press
- 1288 [37] Garcia FE, Bray JD (2018a) Distinct element simulations of shear rupture in dilatant granular  
1289 media. International Journal of Geomechanics, 18(9):04018111
- 1290 [38] Garcia FE, Bray JD (2018b) Distinct element simulations of earthquake fault rupture through  
1291 materials of varying density. Soils and Foundations, 58(4):986-1000
- 1292 [39] Hazeghian M, Soroush A (2015) DEM simulation of reverse faulting through sands with the aid of  
1293 GPU computing. Computers and Geotechnics, 66:253-263.



- 1294 [40] Garcia FE, Bray JD (2019a) Discrete element analysis of earthquake fault rupture-soil-foundation  
1295 interaction. *Journal of Geotechnical and Geoenvironmental Engineering*, 145(9):04019046
- 1296 [41] Garcia FE, Bray JD (2019b) Discrete-element analysis of influence of granular soil density on  
1297 earthquake surface fault rupture interaction with rigid foundations. *Journal of Geotechnical and*  
1298 *Geoenvironmental Engineering*, 145(11): 04019093.
- 1299 [42] Kawamoto R, Andò E, Viggiani G, Andrade JE (2016) Level set discrete element method for three-  
1300 dimensional computations with triaxial case study. *Journal of the Mechanics and Physics of*  
1301 *Solids*, 91:1-13
- 1302 [43] Kawamoto R, Andò E, Viggiani G, Andrade JE (2018) All you need is shape: Predicting shear  
1303 banding in sand with LS-DEM. *Journal of the Mechanics and Physics of Solids*, 111:375-392
- 1304 [44] Harmon JM, Karapiperis K, Li L, Moreland S, Andrade JE (2021) Modeling connected granular  
1305 media: Particle bonding within the level set discrete element method. *Computer Methods in Applied*  
1306 *Mechanics and Engineering*, 373:113486.
- 1307 [45] Silva Dos Santos AP, Consoli NC, Baudet BA (2010) The mechanics of fibre-reinforced sand.  
1308 *Géotechnique*, 60(10):791–799.
- 1309 [46] Li M, He H, Senetakis K (2017) Behavior of carbon fiber-reinforced recycled concrete aggregate.  
1310 *Geosynthetics International*, 24(5):480-490.
- 1311 [47] Fu R, Baudet BA, Madhusudhan BN, Coop MR (2018) A comparison of the performances of  
1312 polypropylene and rubber fibers in completely decomposed granite. *Geotextiles and Geomembranes*,  
1313 46(1):22-28.
- 1314 [48] Madhusudhan BN, Baudet BA, Ferreira PMV, Sammonds P (2017) Performance of fiber  
1315 reinforcement in completely decomposed granite. *Journal of Geotechnical and Geoenvironmental*  
1316 *Engineering*, 143(8): 1-11.
- 1317 [49] Ekinici A (2019) Effect of preparation methods on strength and microstructural properties of  
1318 cemented marine clay. *Construction and Building Materials*, 227:116690.
- 1319 [50] Hight DW, Ellison RA, Page DP (2004) *Engineering in the Lambeth Group London*: Ciria.
- 1320 [51] Hight DW, Gasparre A, Nishimura S, Minh NA, Jardine RJ, Coop MR (2007) Characteristics of the  
1321 London clay from the Terminal 5 site at Heathrow Airport. *Géotechnique*, 57(1):3–18.
- 1322 [52] Skempton AW, Petley DJ (1967) The strength along structural discontinuities in stiff clays. In  
1323 *Proceedings of the Geotechnical Conference Oslo, Norway*: pp 29–45.

- 1324 [53] Marsland A (1971) The shear strength of stiff fissured clays. In Proceedings of the Roscoe  
1325 Memorial Symposium Cambridge, UK: 59–68.
- 1326 [54] Gasparre A, Hight DW, Nishimura S, Minh NA, Jardine RJ, Coop MR (2007) The influence of  
1327 structure on the behaviour of London Clay. *Géotechnique*, 57(1):19–31
- 1328 [55] Vitone C, Cotecchia F (2011) The influence of intense fissuring on the mechanical behaviour of  
1329 clays. *Géotechnique*, 61(12):1003–1018.
- 1330 [56] Fearon RE, Coop MR (2002) The influence of landsliding on the behaviour of a structurally complex  
1331 clay. *Quarterly Journal of Engineering Geology and Hydrogeology*, 35(1):25–32.
- 1332 [57] Fonseca J (2011) The evolution of morphology and fabric of a sand during shearing. Dissertation,  
1333 Imperial College London, London, England, UK.
- 1334 [58] Shire T, O'Sullivan C (2016) Constriction size distributions of granular filters: A numerical  
1335 study. *Géotechnique*, 66(10):826-839.
- 1336 [59] Shire T, O'Sullivan C (2017) A network model to assess base-filter combinations. *Computers and  
1337 Geotechnics*, 84:117-128.
- 1338 [60] Kenney TC, Chahal R, Chiu E, Ofoegbu GI, Omenge GN, Ume CA (1985) Controlling constriction  
1339 sizes of granular filters. *Canadian Geotechnical Journal*, 22(1):32-43.
- 1340 [61] Anselmucci F, Andó E, Sibille L, Lenoir N, Peyroux R, Arson C, Bengough AG (2019) Root-reinforced  
1341 sand: Kinematic response of the soil. In Proceedings of the 7th International Symposium on  
1342 Deformation Characteristics of Geomaterials, IS-Glasgow, EDP Sciences, pp 12011
- 1343 [62] Kim SY, Park J, Cha W, Lee JS, Carlos Santamarina, J (2021) Soil response during globally drained  
1344 and undrained freeze–thaw cycles under deviatoric loading. *Journal of Geotechnical and  
1345 Geoenvironmental Engineering*, 147(2):06020030.
- 1346 [63] Fonseca J, Riaz A, Bernal-Sanchez J, Barreto D, McDougall J, Miranda-Manzanares M, Marinelli A,  
1347 Dimitriadi V (2019) Particle-scale interactions and energy dissipation mechanisms in sand–rubber  
1348 mixtures. *Géotechnique Letters*, 9(4):263-268
- 1349 [64] Stamati O, Andò E, Roubin E, Cailletaud R, Wiebicke M, Pinzon G, Birmipilis G (2020) spam:  
1350 Software for Practical Analysis of Materials. *Journal of Open Source Software*, 5(51):2286.
- 1351 [65] Ghadr S, Bahadori H, Assadi-Langroudi A (2019) Anisotropy in sand–fibre composites and  
1352 undrained stress–strain implications. *International Journal of Geosynthetics and Ground  
1353 Engineering*, 5(3):1-13.

- 1354 [66] Mandolini A, Diambra A and Ibraim E (2019) Strength anisotropy of fibre-reinforced sands under  
1355 multiaxial loading. *Géotechnique*, 69(3):203-216.
- 1356 [67] Mirzababaei M, Anggraini V, Haque A (2020) X-ray computed tomography imaging of fibre-  
1357 reinforced clay subjected to triaxial loading. *Geosynthetics International*, 27(6):635-645.
- 1358 [68] Mirzababaei M, Mohamed M, Miraftab M (2017) Analysis of strip footings on fiber-reinforced  
1359 slopes with the aid of particle image velocimetry. *Journal of Materials in Civil*  
1360 *Engineering*, 29(4):04016243.
- 1361 [69] Wang Y, Hu Y, Hossain MS (2020) Soil flow mechanisms of full-flow penetrometers in layered clays  
1362 through particle image velocimetry analysis in centrifuge test. *Canadian Geotechnical*  
1363 *Journal*, 57(11):1719-1732.
- 1364 [70] Kavazanjian E, van Paassen L (2019) Biogeotechnical mitigation of earthquake-induced soil  
1365 liquefaction. NHERI Workshop, Portland, Oregon, USA.
- 1366 [71] Tang AM, Hughes PN, Dijkstra TA, Askarinejad A, Brenčič M, Cui YJ, Diez JJ, Firgi T, Gajewska B,  
1367 Gentile F, Grossi G, et al. (2018) Atmosphere–vegetation–soil interactions in a climate change context;  
1368 Impact of changing conditions on engineered transport infrastructure slopes in Europe. *Quarterly*  
1369 *Journal of Engineering Geology and Hydrogeology*, 51(2):156-168
- 1370 [72] Yu Z, Eminue OO, Stirling R, Davie C, Glendinning S (2021) Desiccation cracking at field scale on a  
1371 vegetated infrastructure embankment. *Géotechnique Letters*, 11(1):88-95.
- 1372 [73] Emadi-Tafti M, Ataie-Ashtiani B (2019) A modeling platform for landslide stability: A hydrological  
1373 approach. *Water*, 11(10):2146.
- 1374 [74] Tagarelli V (2019) Analysis of the Slope-Vegetation-Atmosphere Interaction for the Design of the  
1375 Mitigation Measures of Landslide Risk in Clayey Slopes. PhD Dissertation, Politecnico di Bari, Bari, Italy.
- 1376 [75] Cotecchia F, Tagarelli V, Pedone G, Ruggieri G, Guglielmi S, Santaloia F (2019) Analysis of climate-  
1377 driven processes in clayey slopes for early warning system design. *Proceedings of the Institution of*  
1378 *Civil Engineers - Geotechnical Engineering*, 172(6):465-480.
- 1379 [76] Cotecchia F, Pedone G, Bottiglieri O, Santaloia F, Vitone C (2014) Slope-atmosphere interaction in  
1380 a tectonized clayey slope: A case study. *Italian Geotechnical Journal*, 1(14):34-61.
- 1381 [77] Evans JR (1989) Photosynthesis and nitrogen relationships in leaves of C3 plants. *Oecologia* 78:9-  
1382 19.

- 1383 [78] Flexas J, Medrano H (2002) Drought-inhibition of photosynthesis in C3 plants: stomatal and non-  
1384 stomatal limitations revisited. *Ann. Bot.*, 89:183-189.
- 1385 [79] Tagarelli V, Cotecchia F (2020) Deep Movements in Clayey Slopes Relating to Climate: Modeling  
1386 for Early Warning System Design. *Research for Land Protection and Development. CNRIG 2019. Lect.*  
1387 *Notes Civil Eng.* 40.
- 1388 [80] Tagarelli V, Cotecchia F. (2020) The Effects of Slope Initialization on the Numerical Model  
1389 Predictions of the Slope-Vegetation-Atmosphere Interaction. *Geosciences*, 10:85.
- 1390 [81] Ghannoum O (2009) C4 photosynthesis and water stress. *Ann Bot.*, 103(4):635-44. doi:  
1391 10.1093/aob/mcn093.
- 1392 [82] Christin PA, Osborne CP (2014) The evolutionary ecology of C4 plants. *New Phytologist*,  
1393 204(4):765–781. doi:10.1111/nph.13033.
- 1394 [83] Hogan CM (2011) Respiration. *Encyclopaedia of Earth*. In McGinley M, Cleveland CJ (Ed). National  
1395 Council for Science and the Environment. Washington, D.C.
- 1396 [84] Sage RF, Sage TL, Kocacinar F (2012) Photorespiration and the evolution of C4 photosynthesis.  
1397 *Annual Review of Plant Biology*, 63(1):19–47. doi:10.1146/annurev-arplant-042811-105511.
- 1398 [85] Tagarelli (2021) Preliminary field data of selected deep-rooted vegetation effects on the slope-  
1399 vegetation-atmosphere interaction: Results from an in-situ test. In *First NiSE Workshop (NiSE1)*, 11-12  
1400 February, University of East London, London, UK.
- 1401 [86] Neris J, Jiménez C, Fuentes J, Morillas G, Tejedor M (2012) Vegetation and land-use effects on soil  
1402 properties and water infiltration of Andisols in Tenerife (Canary Islands, Spain). *CATENA*, 98:55-62.
- 1403 [87] Wang C, Zhao C, Xu Z, et al. (2013) Effect of vegetation on soil water retention and storage in a  
1404 semi-arid alpine forest catchment. *J. Arid Land*, 5:207-219. [https://doi.org/10.1007/s40333-013-0151-](https://doi.org/10.1007/s40333-013-0151-5)  
1405 5
- 1406 [88] Leung AK, Garg A, Ng CWW (2015) Effects of plant roots on soil-water retention and induced  
1407 suction in vegetated soil. *Engineering Geology*, 193:183–197. doi:10.1016/j.enggeo.2015.04.017
- 1408 [89] Ivanov V, Stabnikov V (2016) *Construction Biotechnology: Biogeochemistry, Microbiology and*  
1409 *Biotechnology of Construction Materials and Processes*. Springer.
- 1410 [90] Hatch H (2020) Bryce Canyon City, UT, USA. <https://unsplash.com/photos/QJ0rRpumcVM>  
1411 Accessed 09 July 2021.

- 1412 [91] Leonardi S (2020) Arches National Park, Utah, USA. <https://unsplash.com/photos/1UWJt8glpt8>  
1413 Accessed 09 July 2021.
- 1414 [92] Sahatchiev H (2019) Belogradchik, Vidin, Bulgaria. <https://unsplash.com/photos/iQS2BCfHc10>  
1415 Accessed 09 July 2021.
- 1416 [93] Ivanov V (2011) Environmental Microbiology for Engineers. CRC press.
- 1417 [94] Ivanov V, Stabnikov V, Kawasaki S (2019) Ecofriendly calcium phosphate and calcium bicarbonate  
1418 biogrouts. Journal of Cleaner Production, 218:328-334.
- 1419 [95] Berlanga M, Guerrero R (2016) Living together in biofilms: The microbial cell factory and its  
1420 biotechnological implications. Microbial Cell Factories, 15(1):1-11
- 1421 [96] Ta HX (2016) Microbial biofilm in porous sediments: Effects on soil behaviour. PhD Dissertation,  
1422 Washington State University, USA
- 1423 [97] Ta HX, Muhunthan B, Ramezani S, Abu-Lail N, Kwon TH (2017) Effects of bacterial dextran on  
1424 soil geophysical properties. Environmental Geotechnics, 5(2):114-122
- 1425 [98] Fujita Y, Taylor JL, Wendt LM, Reed DW, Smith RW (2010) Evaluating the potential of native  
1426 ureolytic microbes to remediate a 90Sr contaminated environment. Environmental Science and  
1427 Technology, 44(19):7652-7658
- 1428 [99] Ghosh S, Biswas M, Chattopadhyay BD, Mandal S (2009) Microbial activity on the microstructure  
1429 of bacteria modified mortar. Cement and Concrete Composites, 31(2):93-98
- 1430 [100] Cunningham AB, Gerlach R, Spangler L, Mitchell AC (2009) Microbially enhanced geologic  
1431 containment of sequestered supercritical CO<sub>2</sub>. Energy Procedia, 1(1):3245-3252
- 1432 [101] Tobler DJ, Cuthbert MO, Greswell RB, Riley MS, Renshaw JC, Handley-Sidhu S, Phoenix VR (2011)  
1433 Comparison of rates of ureolysis between *Sporosarcina pasteurii* and an indigenous groundwater  
1434 community under conditions required to precipitate large volumes of calcite. Geochimica et  
1435 Cosmochimica Acta, 75(11):3290-3301
- 1436 [102] Krishnan V, Khodadadi Tirkolaei H, Martin K, Hamdan N, van Paassen LA, Kavazanjian Jr E (2021)  
1437 Variability in the unconfined compressive strength of EICP-treated "standard" sand. Journal of  
1438 Geotechnical and Geoenvironmental Engineering, 147(4): 06021001
- 1439 [103] van Paassen (2021) Centre for bio-mediated and bio-inspired geotechnics. In First NiSE  
1440 Workshop (NiSE1), 11-12 February, University of East London, London, UK.

- 1441 [104] Ivanov V, Stabnikov V, Stabnikova O, Kawasaki S (2019) Environmental safety and biosafety in  
1442 construction biotechnology. *World Journal of Microbiology and Biotechnology*, 35(2):26
- 1443 [105] Abbasi B, Ta HX, Muhunthan B, Ramezani S, Abu-Lail N, Kwon TH (2018) Modeling of  
1444 permeability reduction in bioclogged porous sediments. *Journal of Geotechnical and*  
1445 *Geoenvironmental Engineering*, 144(4):06018016
- 1446 [106] El Mountassir, G, Minto JM, van Paassen LA, Salifu E, Lunn RJ (2018) Applications of microbial  
1447 processes in geotechnical engineering. *Advances in Applied Microbiology*, 104:39-91
- 1448 [107] van Paassen LA (2009) Biogrout, Ground Improvement by Microbial Induced Carbonate  
1449 Precipitation. PhD dissertation, TU Delft, The Netherlands
- 1450 [108] van Paassen LA, van Loosdrecht MCM, Pieron M, Mulder A, Ngan-Tillard DJM, van der Linden  
1451 TJM (2010) Strength and deformation of biologically cemented sandstone, In Vrkljan (ed), *I Rock*  
1452 *Engineering in Difficult Ground Conditions – Soft Rocks and Karst*, pp 405-410
- 1453 [109] van Paassen LA, Ghose R, van der Linden TJ, van der Star WR, van Loosdrecht MC (2010)  
1454 Quantifying biomediated ground improvement by ureolysis: Large-scale biogrout experiment. *Journal*  
1455 *of Geotechnical and Geoenvironmental Engineering*, 136(12):1721-1728
- 1456 [110] Shahrokhi-Shahraki R, Zomorodian SMA, Niazi A, O'Kelly BC (2015) Improving sand with  
1457 microbial-induced carbonate precipitation. *Proceedings of the Institution of Civil Engineers-Ground*  
1458 *Improvement*, 168(3):217-230. <https://doi.org/10.1680/grim.14.00001>
- 1459 [111] Minto JM, Hingerl FF, Benson SM, Lunn RJ (2017) X-ray CT and multiphase flow characterization  
1460 of a 'bio-grouted' sandstone core: The effect of dissolution on seal longevity. *International Journal of*  
1461 *Greenhouse Gas Control*, 64:152-162
- 1462 [112] Burbank MB, Weaver TJ, Williams BC, Crawford RL (2012) Urease activity of ureolytic bacteria  
1463 isolated from six soils in which calcite was precipitated by indigenous  
1464 bacteria. *Geomicrobiology*, 29(4):389-395
- 1465 [113] Svirčev Z, Marković SB, Stevens T, Codd GA, Smalley I, Simeunović J, Obreht I, Dulić T, Pantelić  
1466 D, Hambach U (2013) Importance of biological loess crusts for loess formation in semi-arid  
1467 environments. *Quaternary International*, 296:206-215.
- 1468 [114] De Jong JT, Soga KS, Kavazanjian E, Burns S, van Paassen LA, Al Quabany A, Aydilek A, Bang SS,  
1469 Burbank M, Caslake LF, Chen CY, Cheng X, Chu J, Ciurli S, Esnault-Filet A, Fauriel S, Hamdan N, Hata T,  
1470 Inagaki Y, Jefferis S, Kuo M, Laloui L, Larrahondo J, Manning DAC, Martinez B, Montoya BM, Nelson  
1471 DC, Palomino A, Renforth P, Santamarina JC, Seagren EA, Tanyu B, Tsesarsky M, Weaver T (2013)

- 1472 Biogeochemical processes and geotechnical applications: Progress, opportunities and  
 1473 challenges. *Géotechnique*, 63(4):287-301
- 1474 [115] Amin M, Zomorodian SMA, O'Kelly BC (2017) Reducing the hydraulic erosion of sand using  
 1475 microbial-induced carbonate precipitation. *Proceedings of the Institution of Civil Engineers-Ground  
 1476 Improvement*, 170(2):112-122. <https://doi.org/10.1680/jgrim.16.00028>
- 1477 [116] Zomorodian SMA, Ghaffari H, O'Kelly BC (2019) Stabilisation of crustal sand layer using  
 1478 biocementation technique for wind erosion control. *Aeolian Research*, 40:34-41.  
 1479 <https://doi.org/10.1016/j.aeolia.2019.06.001>
- 1480 [117] Haouzi FZ, Courcelles B (2018) Major applications of MICP sand treatment at multi-scale levels:  
 1481 A review. In *Proceedings of GeoEdmonton 2018: The 71st Canadian Geotechnical Conference and The  
 1482 13th Joint CGS/IAH-CNC Groundwater Conference*.
- 1483 [118] Esnault-Filet A, Mosser JF, Monleau S, Sapin L, Gutjahr I (2015) Prix de l'Innovation Solscope:  
 1484 Biocalcis. Public technical report: [https://www.solscope.fr/medias/MEMOIRE-TECHNIQUE-Biocalcis-  
 1485 Version-publique-.pdf](https://www.solscope.fr/medias/MEMOIRE-TECHNIQUE-Biocalcis-Version-publique-.pdf)
- 1486 [119] Guyet A, Dade-Robertson M, Wipat A, Casement J, Smith W, Mitrani H, Zhang M (2018) Mild  
 1487 hydrostatic pressure triggers oxidative responses in *Escherichia coli*. *PloS One*, 13(7), pe0200660
- 1488 [120] Arnardottir TH, Dade-Robertson M, Mitrani H, Zhang M, Christgen B (2021), Turbulent Casting:  
 1489 Bacterial Expression in Mineralized Structures. In *ACADIA Association for Computer Aided Design in  
 1490 Architecture*
- 1491 [121] Handley-Sidhu S, Sham E, Cuthbert MO, Nougazol S, Mantle M, Johns ML, Macaskie LE, Renshaw  
 1492 JC (2013) Kinetics of urease mediated calcite precipitation and permeability reduction of porous media  
 1493 evidenced by magnetic resonance imaging. *International Journal of Environmental Science and  
 1494 Technology*, 10(5):881-890
- 1495 [122] Kavazanjian E, Hamdan N (2015) Enzyme induced carbonate precipitation (EICP) columns for  
 1496 ground improvement. In *IFCEE 2015*, pp 2252-2261
- 1497 [123] Martin KK, Khodadadi TH, Kavazanjian Jr, E (2020) Enzyme-induced carbonate precipitation:  
 1498 Scale-up of bio-cemented soil columns. In *Geo-Congress 2020: Biogeotechnics*, Reston, VA: ASCE, pp  
 1499 96-103.
- 1500 [124] Wang L, van Paassen L, Gao Y, He J, Gao Y, Kim D (2020) Laboratory tests on mitigation of soil  
 1501 liquefaction using microbial induced desaturation and precipitation. *Geotechnical Testing  
 1502 Journal*, 44(2):520-534

- 1503 [125] O'Donnell ST, Rittmann BE, Kavazanjian Jr E (2017) MIDP: Liquefaction mitigation via microbial  
1504 denitrification as a two-stage process I: Desaturation. *Journal of Geotechnical and Geoenvironmental*  
1505 *Engineering*, 143(12):04017094
- 1506 [126] Khosravifar A, Moug D (2019) Liquefaction mitigation in silts using microbially induced  
1507 desaturation. Portland State University
- 1508 [127] Tan L, Reeksting B, Ferrandiz-Mas V, Heath A, Gebhard S, Paine K (2020) Effect of carbonation  
1509 on bacteria-based self-healing of cementitious composites. *Construction and Building*  
1510 *Materials*, 257:119501
- 1511 [128] Litina C, Al-Tabbaa A (2020) First generation microcapsule-based self-healing cementitious  
1512 construction repair materials. *Construction and Building Materials*, 255:119389
- 1513 [129] Botusharova S, Gardner D, Harbottle M (2020) Augmenting microbially induced carbonate  
1514 precipitation of soil with the capability to self-heal. *Journal of Geotechnical and Geoenvironmental*  
1515 *Engineering*, 146(4):04020010
- 1516 [130] Chen C, Wu L, Harbottle M (2020) Exploring the effect of biopolymers in near-surface soils using  
1517 xanthan gum–modified sand under shear. *Canadian Geotechnical Journal*, 57(8):1109-1118
- 1518 [131] Chang I, Lee M, Tran ATP, Lee S, Kwon YM, Im J, Cho GC (2020) Review on biopolymer-based soil  
1519 treatment (BPST) technology in geotechnical engineering practices. *Transportation*  
1520 *Geotechnics*, 24:100385.
- 1521 [132] Khatami HR, O'Kelly BC (2013) Improving mechanical properties of sand using  
1522 biopolymers. *Journal of Geotechnical and Geoenvironmental Engineering*, 139(8):1402-1406.  
1523 [https://doi.org/10.1061/\(ASCE\)GT.1943-5606.0000861](https://doi.org/10.1061/(ASCE)GT.1943-5606.0000861)
- 1524 [133] Ni J, Li SS, Ma L, Geng, XY (2020) Performance of soils enhanced with eco-friendly biopolymers  
1525 in unconfined compression strength tests and fatigue loading tests. *Construction and Building*  
1526 *Materials*, 263:120039
- 1527 [134] Chang I, Im J, Cho GC (2016) Geotechnical engineering behaviors of gellan gum biopolymer  
1528 treated sand. *Canadian Geotechnical Journal*, 53(10):1658-1670
- 1529 [135] Khatami HR, O'Kelly BC (2018) Prevention of bleeding of particulate grouts using  
1530 biopolymers. *Construction and Building Materials*, 192:202-209.  
1531 <https://doi.org/10.1016/j.conbuildmat.2018.10.131>



- 1532 [136] Geng X (2021) Eco-friendly ground improvement techniques for transport infrastructure  
 1533 earthwork. In First NiSE Workshop (NiSE1), 11-12 February, University of East London, London, UK.
- 1534 [137] Tarantino A, El Mountassir G, Wheeler S, Gallipoli D, Russo G, Augarde C, Urciuoli G, Pirone M,  
 1535 Stokes A, van de Kuilen JW, Gard W (2020) TERRE project: Interplay between unsaturated soil  
 1536 mechanics and low-carbon geotechnical engineering
- 1537 [138] Salifu E, El Mountassir G (2020) Fungal-induced water repellency in sand. *Géotechnique*,  
 1538 71(7):608-615.
- 1539 [139] Fraccica A, Romero Morales EE, Fourcaud T (2019) Multi-scale effects on the hydraulic behaviour  
 1540 of a root-permeated and compacted soil. IS-Glasgow 2019–7th International Symposium on  
 1541 Deformation Characteristics of Geomaterials, EDP Sciences, pp 1-5.
- 1542 [140] Salifu, E, El Mountassir, G, Minto, J. M. and Tarantino, A. (2021) Hydraulic behaviour of fungal  
 1543 treated sand, *Geomechanics for Energy and the Environment*,  
 1544 <https://doi.org/10.1016/j.gete.2021.100258>
- 1545 [141] Milodowski AE, Northmore KJ, Kemp SJ et al. (2015) The mineralogy and fabric of ‘Brickearths’  
 1546 in Kent, UK and their relationship to engineering behaviour. *Bull Eng Geol Environ*, 74:1187–1211.  
 1547 <https://doi.org/10.1007/s10064-014-0694-5>
- 1548 [142] Jamsawang P, Suansomjeen T, Sukontasukkul P, Jongpradist P, Bergado DT (2018) Comparative  
 1549 flexural performance of compacted cement-fiber-sand. *Geotextiles and Geomembranes*, 46(4):414-  
 1550 425. doi: 101016/j.geotexmem201803008
- 1551 [143] Tang C, Shi B, Gao W, Chen F, Cai Y (2007) Strength and mechanical behavior of short  
 1552 polypropylene fiber reinforced and cement stabilized clayey soil. *Geotextiles and Geomembranes*,  
 1553 25(3): 194–202 doi: 101016/j.geotexmem200611002
- 1554 [144] Botero E, Ossa A, Sherwell G, Ovando-Shelley E (2015) Stress-strain behavior of a silty soil  
 1555 reinforced with polyethylene terephthalate (PET). *Geotextiles and Geomembranes*, 43(4):363-369 doi:  
 1556 101016/j.geotexmem201504003
- 1557 [145] Yi XW, Ma GW, Fourie A (2015) Compressive behaviour of fibre-reinforced cemented paste  
 1558 backfill. *Geotextiles and Geomembranes*, 43(3):207-215 doi: 101016/j.geotexmem201503003.
- 1559 [146] Özkul ZH, Baykal G (2007) Shear behavior of compacted rubber fiber-clay composite in drained  
 1560 and undrained loading. *Journal of Geotechnical and Geoenvironmental Engineering*, 133(7): 767–781  
 1561 doi: 101061/(ASCE)1090-0241(2007)133:7(767)

- 1562 [147] Mirzababaei M, Arulrajah A, Horpibulsuk S, Aldava M (2017) Shear strength of a fibre-reinforced  
1563 clay at large shear displacement when subjected to different stress histories. *Geotextiles and*  
1564 *Geomembranes*, 45(5):422-429
- 1565 [148] Tang CS, Li J, Wang DY, Shi B (2016) Investigation on the interfacial mechanical behavior of wave-  
1566 shaped fiber reinforced soil by pullout test. *Geotextiles and Geomembranes*, 44(6):872-883 doi:  
1567 101016/jgeotextmem201605001
- 1568 [149] Ayeldeen M, Kitazume M (2017) Using fiber and liquid polymer to improve the behaviour of  
1569 cement-stabilized soft clay. *Geotextiles and Geomembranes*, 45(6):592-602 doi:  
1570 101016/jgeotextmem201705005
- 1571 [150] Li Y, Mai YW, Ye L (2005) Effects of fibre surface treatment on fracture-mechanical properties of  
1572 sisal-fibre composites. *Composite Interfaces*, 12(1-2):141-163 doi: 101163/1568554053542151
- 1573 [151] Li C, Zornberg JG (2019) Shear strength behavior of soils reinforced with weak fibers. *Journal of*  
1574 *Geotechnical and Geoenvironmental Engineering*, 145(9):2-8 doi: 101061/(ASCE)GT1943-  
1575 56060002109
- 1576 [152] Li C, Zornberg JG (2013) Mobilization of reinforcement forces in fiber-reinforced soil. *Journal of*  
1577 *Geotechnical and Geoenvironmental Engineering*, 139(1):107-115 doi: 101061/(ASCE)GT1943-  
1578 56060000745
- 1579 [153] Ekinci A, Ferreira PMV (2012) The undrained mechanical behaviour of a fibre-reinforced heavily  
1580 over-consolidated clay. *ISSMGE - TC 211 International Symposium on Ground Improvement, Brussels,*  
1581 *Belgium.*
- 1582 [154] Wang YX, Guo PP, Ren WX, Yuan BX, Yuan HP, Zhao YL, Shan SB, Cao P (2017) Laboratory  
1583 investigation on strength characteristics of expansive soil treated with jute fiber  
1584 reinforcement. *International Journal of Geomechanics*, 17(11):04017101
- 1585 [155] Mirzababaei M, Arulrajah A, Horpibulsuk S, Soltani A, Khayat N (2018) Stabilization of soft clay  
1586 using short fibers and poly vinyl alcohol. *Geotextiles and Geomembranes*, 46(5):646-655.
- 1587 [156] Mirzababaei M, MirafTAB M, Mohamed M, McMahon P (2013) Unconfined compression strength  
1588 of reinforced clays with carpet waste fibers. *Journal of Geotechnical and Geoenvironmental*  
1589 *Engineering*, 139(3):483-493
- 1590 [157] Assadi-Langroudi A, Ghadr S, Theron E, Oderinde SA, Katsipatakis EM (2019) Lime cake as an  
1591 alternative stabiliser for loose clayey loams. *International Journal of Geosynthetics and Ground*  
1592 *Engineering*, 5(3):1-13

- 1593 [158] Mirzababaei M (2021), Advances in soil fibre reinforcement. In First NiSE Workshop (NiSE1),  
1594 11-12 February, University of East London, London, UK.
- 1595 [159] Assadi-Langroudi A (2021) On mechanics of porous granular matters. In First NiSE Workshop  
1596 (NiSE1), 11-12 February, University of East London, London, UK.
- 1597 [160] Pye K (1987) Eolian Dust and Dust Deposits. London, Academic Press
- 1598 [161] Krinsley DH, Doornkamp JC (1973) Atlas of Quartz Sand Surface Textures. London, Syndics of the  
1599 Cambridge University Press
- 1600 [162] Ghadr S, Assadi-Langroudi A, Hung C, O’Kelly BC, Bahadori H, Ghodsi T (2020) Stabilization of  
1601 sand with colloidal nano-silica hydrosols. Applied Sciences, 10(15):5192.  
1602 <https://doi.org/10.3390/app10155192>
- 1603 [163] Ghadr S, Assadi-Langroudi A, Hung C (2020) Stabilisation of peat with colloidal nanosilica. Mires  
1604 and Peat: 26(Art 9)
- 1605 [164] Kua TA, Arulrajah A, Mohammadinia A, Horpibulsuk S, Mirzababaei M (2017) Stiffness and  
1606 deformation properties of spent coffee grounds based geopolymers. Construction and Building  
1607 Materials, 138:79-87.
- 1608 [165] Arulrajah A, Yaghoubi M, Disfani MM, Horpibulsuk S, Bo MW, Leong M (2018) Evaluation of fly  
1609 ash-and slag-based geopolymers for the improvement of a soft marine clay by deep soil mixing. Soils  
1610 and Foundations, 58(6):1358-1370
- 1611 [166] Horpibulsuk S, Phetchuay C, Chinkulkijniwat A (2012) Soil stabilization by calcium carbide residue  
1612 and fly ash. Journal of Materials in Civil Engineering, 24(2):184-193
- 1613 [167] Hoy M, Horpibulsuk S, Arulrajah A (2016) Strength development of recycled asphalt pavement–  
1614 fly ash geopolymer as a road construction material. Construction and Building Materials, 117:209-219
- 1615 [168] Shekhawat P, Sharma G, Singh RM (2020) Potential application of heat cured eggshell powder  
1616 and fyash-based geopolymer in pavement construction. International Journal of Geosynthetics and  
1617 Ground Engineering, 6(2):1-17.
- 1618 [169] Dade-Robertson M, Mitrani H, Rodriguez-Corral J, Zhang M, Hernan L, Guyet A, Wipat A (2018)  
1619 Design and modelling of an engineered bacteria-based pressure-sensitive soil. Bioinspiration and  
1620 Biomimetics 13(4):046004

1621 [170] Rodriguez Corral J, Mitrani H, Dade-Robertson M, Zhang M, Maiello P (2020) Agarose gel as a  
1622 soil analogue for development of advanced bio-mediated soil improvement methods. Canadian  
1623 Geotechnical Journal, 57(12):2010-2019

1624 [171] Dade-Robertson M, Corral JR, Mitrani H, Zhang M, Wipat A, Ramirez-Figueroa C, Hernan L (2016)  
1625 Thinking Soils: a synthetic biology approach to material-based design computation ACADIA

1626 [172] Hodaie M, Maghoul P, Popplewell N (2020) An overview of the acoustic studies of bone-like  
1627 porous materials, and the effect of transverse acoustic waves. International Journal of Engineering  
1628 Science, 147: 103189

1629 [173] Liu H, Maghoul P, Shalaby A (2020) Laboratory-scale characterization of saturated soil samples  
1630 through ultrasonic techniques. Nature Scientific Reports, 10, 3216.

1631 [174] Liu H, Maghoul P, Shalaby A (2021) A poro-elastodynamic forward solver for dispersion analysis  
1632 of saturated multilayer systems. In Barla M, Di Donna A, Sterpi D (Eds). Challenges and Innovations in  
1633 Geomechanics. IACMAG 2021. Lecture Notes in Civil Engineering. 126:637-644

1634

1635

1636

1637

1638

1639

1640

1641

1642

1643

1644

1645

1646

1647

1648 **List of Figures**

1649 **Fig. 1** (a) NiSE five principal aims and interlinked deliverables; (b) NiSE deliverables as indicators of  
 1650 materials' performance, measured by a traffic-light scoring system: the framework can be applied to  
 1651 candidate stabilising materials in any project

1652

1653 **Fig. 2** Qualitative picture of aggregation during MD simulations; Clay platelets' orientations according  
 1654 to the  $\varphi$  angle ( $0^\circ$  representing alignment of normal vector of platelets with the z axis) [14]

1655

1656 **Fig. 3** Simulation of uniaxial compression of highly porous particulate matters through importing the  
 1657 "diffusion-limited aggregation" algorithm into 3D DEM software package PFC3D [11]

1658

1659 **Fig. 4** Left: aluminium die casting and significance of identifying areas of potential weakness [15];  
 1660 Right: coupled LBM-DEM simulations and time-resolved synchrotron X-ray radiography applied to  
 1661 the study of complex stress-strain behaviour of globular Al-Cu alloys and links to critical-state soil  
 1662 mechanics [12]

1663

1664 **Fig. 5** Examples of molecular modelling and their application in geomechanics in the context of NiSE:  
 1665 (a) molecular dynamics (MD) simulation of minimized and equilibrated kerogen-calcite system that is  
 1666 useful for calculating the non-bonded interactions between the organic matter and calcite in porous  
 1667 soils ([23] – with some modifications); (b) variation of shear strain (creep) with potential energy  
 1668 against number of loading/unloading cycles in C-S-H [26]; (c-d) crystal structure and forcefield for a  
 1669 complex multi-body NS-kaolinite-sulphates system [25]

1670

1671 **Fig. 6** For threshold fines content of 30 to 40%: (a) maximum static flow potential [45]; (b) equal  
 1672 idealised micro- and macro-void ratios [35]; (c) changing fabric from RLP to RCP as fines content  
 1673 increases beyond the 30 to 40% threshold [32 – with permission from ASCE]; (d) maximum  
 1674 liquefaction risk [35]

1675

1676 **Fig. 7** DEM-DFD coupled simulation for a gap-graded material showing the greater ability of fines to  
 1677 transmit effective stress through the pore network [36]

1678

1679 **Fig. 8** Typical microcomputed tomography laboratory setup [14]

1680

1681 **Fig. 9** (a) Example of a network model for simulating the migration of base particles (e.g., clay, nano-  
 1682 stabilising agent, biopolymer nuclei) through the network, where the size of the edge of the network  
 1683 is determined from CSD, informed by  $\mu$ CT [59]; (b) Criteria, whether a base particle would move  
 1684 through the constriction, whether it would be trapped, and when it would be retained in the void  
 1685 space [59]; (c) An example of determining CSD as a function of 15% percentile of particle size [58]

1686

1687 **Fig. 10** Interior of the X-ray chamber accommodating miniature triaxial cell [70]

1688

1689 **Fig. 11** Reconstructed 3D greyscale images of triaxial mini-specimen at three axial strains and three  
1690 views (XY, XZ and 3D), followed by spatial distribution of fibres and 3D distribution of fibre  
1691 orientation and length at three axial strains (reproduced from [70])

1692

1693 **Fig. 12** Soil flow mechanism as a T-bar penetrates stiff clay and pushes through an underlying soft clay  
1694 stratum –  $D_i$  is the bar diameter;  $d$  is its vertical displacement and  $x$  is its horizontal displacement [69].

1695

1696 **Fig. 13** (a) BIONICS research embankment, in northern England, covered to the north with grasses  
1697 (e.g., *Alopecurus pratense* and *Lolium perenne*) and to the south with wildflowers (e.g., *Leucanthemum*  
1698 *vulgare*, *Filipendula ulmaria*, *Achillea millefolium* and *Knautia arvensis*). Instrumentations allow  
1699 measurement of volumetric water content, electrical conductivity and soil temperature [72]; (b)  
1700 Pisciollo hillslope in southern Italy covered with (c) C3-cycle *leguminous* and (d) C4-cycle *Gramineae*  
1701 plants [85]

1702

1703 **Fig. 14** Signatures of natural biocementation in sandstone: (a) Bryce Canyon National Park, Utah, USA  
1704 [90]; (b) Arches National Park, Utah, USA [91]; (c) The Belogradchik, Vidin, Bulgaria [92]

1705

1706 **Fig. 15** (a): Bacterial life cycle and biofilm formation [95]; (b): possible forms of bacterial growth on  
1707 soil particle surface [105 – with permission from ASCE]; (c): clean Ottawa sand ( $D_{50} = 120 \mu m$ ) packed  
1708 to a void ratio of 0.6 (left), transformed into Dextran-mediated sand (middle), where particles are  
1709 coated and bridged at the cost of a decrease in porosity, and hence permeability [97]

1710

1711 **Fig. 16** MICP trials in three scales: (a) cubic meter sand box [103] – photograph from [117]; (b) 100  
1712 cubic meter sand box [109]; (c) 1000 cubic meter field-scale mediation [103]; (d) MICP at large scale:  
1713 MICP-treated 400-mm dia. column by Soletanche-Bachy [118]

1714

1715 **Fig. 17** 3D visualization of the X-ray CT data illustrating the variation in porosity: (a) pre-MICP  
1716 precipitation; (b) post-MICP precipitation; (c-d) service time under acidic conditions in favour of  $CaCO_3$   
1717 dissolution [111]

1718

1719 **Fig. 18** EICP trials at field-scale: soil column in box test set-up with TAM and packer, and needle  
1720 penetrometer measurements done on cemented soil section [123 – with permission from ASCE]

1721

1722 **Fig. 19** (a-b) MID test setup in Portland, Oregon, USA: injection probe and monitoring installation,  
1723 including cross-hole and downhole TREX sensor array measuring excess porewater pressure,  $V_p$  and

1724  $V_s$ , and CTD divers; (c) measuring fluid volume and salinity, and TEROS-12 sensors; (d) measuring  
1725 salinity and temperature; (e) P- and S-wave velocity cross-hole measurements [126]

1726 **Fig. 20** Comparison between MICP and BPST processes [124]. Note, in Fig. 20c rods represent soil  
1727 particles and red-coloured lines represent biopolymer chains, with adhesive force among themselves  
1728 and cohesive force between them and the soil particles

1729

1730 **Fig. 21** Influence of fungal mycelial networks on soil behaviour: (a) growth of *Pleurotus ostreatus*  
1731 edible fungi in soil; (b-c) growth of fungi in a column of sand; (d) water repellency [140]

1732

1733 **Fig. 22** Consolidated-undrained (CU) behaviour of sands and fibre-reinforced sands under cyclic and  
1734 anisotropic loading conditions (a and b): first and second stress–strain hysteresis loops for two sands,  
1735 mixed with silt and fibre [35]; (c) HCTS CU results for sand, with and without fibre reinforcement,  
1736 showing stress–strain curves for  $p' = 400$  kPa,  $\alpha = 30^\circ$ , and  $b = 0.5$  and  $1.0$  (compression and torsion)  
1737 [65]; (d) HCTS results for sand, with and without fibre reinforcement showing stress–strain curves for  
1738  $p' = 400$  kPa,  $\alpha = 60^\circ$ ,  $b = 0.5$  and  $1.0$  (torsion). Note: HCTS, hollow cylinder torsional shear;  $p'$ , effective  
1739 mean normal stress;  $\alpha$ , principal stress orientation to vertical direction;  $b$ , intermediate principal stress  
1740 ratio [65]

1741

1742 **Fig. 23** Examples of natural, synthetic and recycled fibres sometimes mixed in soil to imitate plant  
1743 rootlet reinforcement effect: (a) coir [158]; (b) nylon – virgin synthetic [158]; (c) polypropylene – virgin  
1744 synthetic [158]; (d) fibreglass – virgin synthetic [158]; (e-f) waste carpet [156]; (g) jute [154 – with  
1745 permission from ASCE]; (h): coir [67]; (i) thermoplastic polymeric microsynthetic [65]; (j) granulated  
1746 tyre [159]

1747

1748 **Fig. 24** Sculpting soil responses to force by altering sequences of DNA and through the interaction of  
1749 many different genetic devices and engineered organisms: (a) artists impression of a bio-based self-  
1750 constructing foundation [170]; (b) unconfined compression performed on a column of agarose gel  
1751 [171]; (c) microstructure of Agarose LM gel [170]; (d) simulation of multilateral flow (growth media  
1752 for bacteria) and implications of 3D architecture of cementation in sands [120]; (e-f) 3D sand forms,  
1753 scanned as excavation takes place, in seeking an insight into cementation process [120]

1754

1755

1756

1757

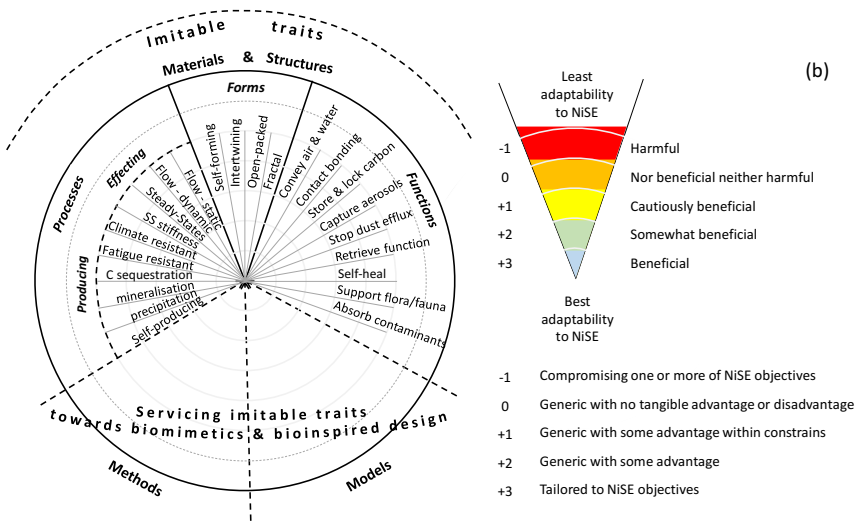
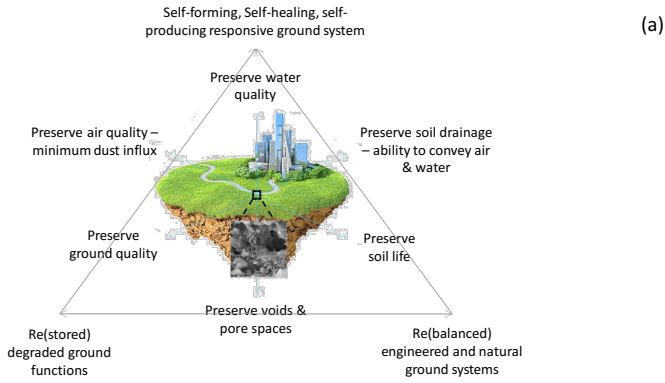
1758

1759

1760

1761

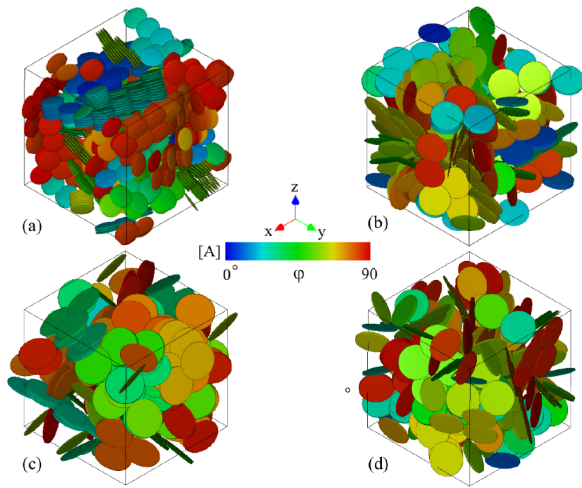
1762 Figure 1



1763  
1764  
1765  
1766  
1767  
1768  
1769



1770 Figure 2



1771

1772

1773

1774

1775

1776

1777

1778

1779

1780

1781

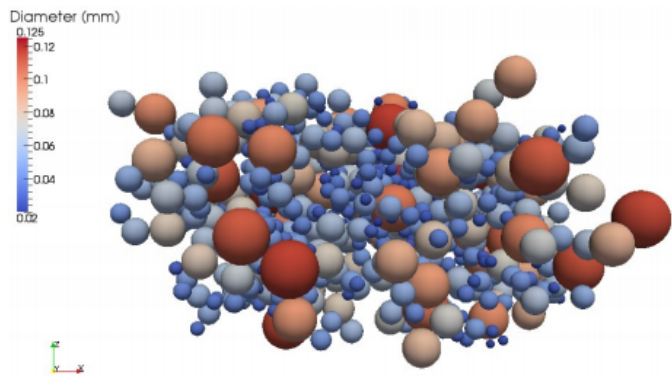
1782

1783

1784

1785

1786 Figure 3



1787

1788

1789

1790

1791

1792

1793

1794

1795

1796

1797

1798

1799

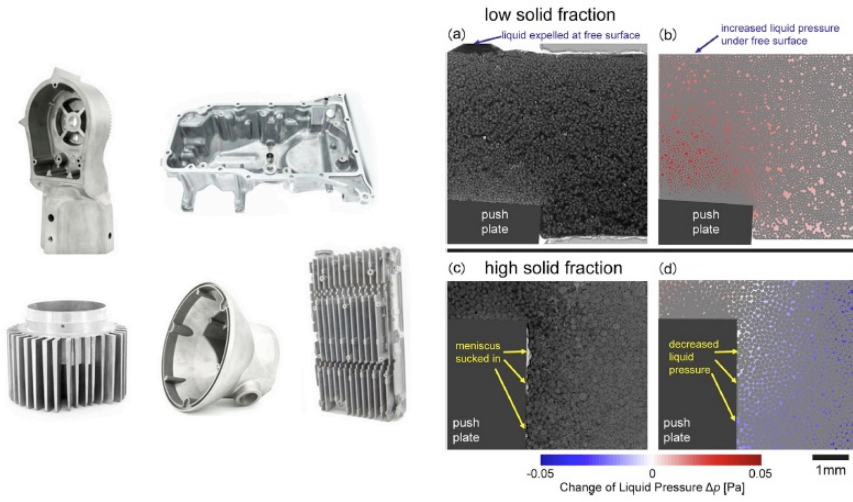
1800

1801

1802

1803

1804 Figure 4



1805

1806

1807

1808

1809

1810

1811

1812

1813

1814

1815

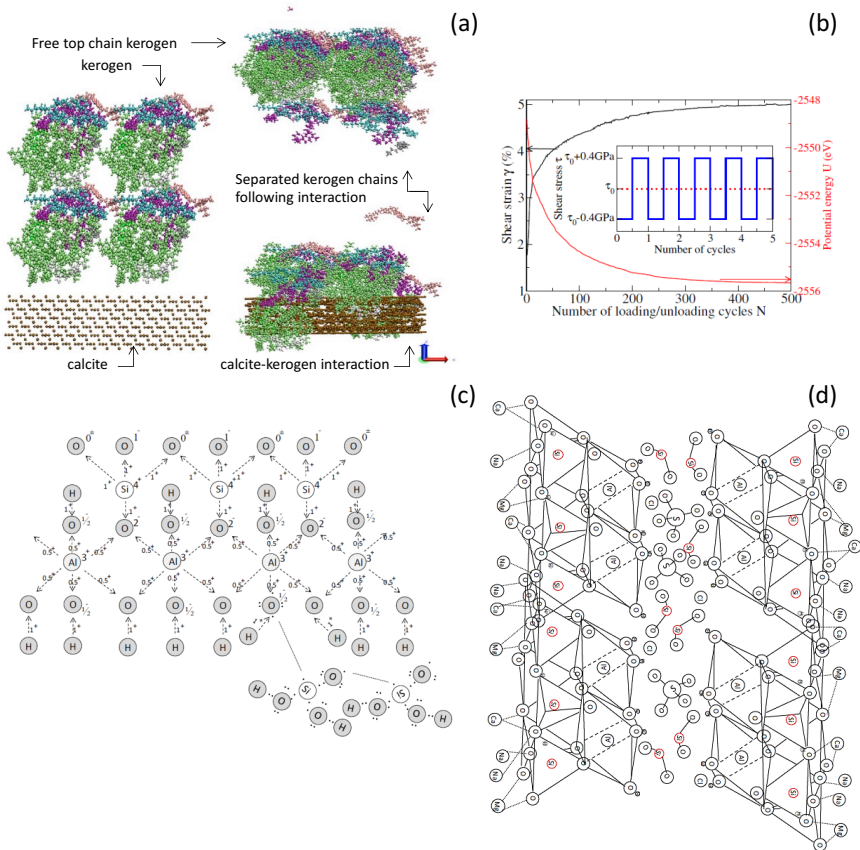
1816

1817

1818

1819

1820 Figure 5



1821

1822

1823

1824

1825

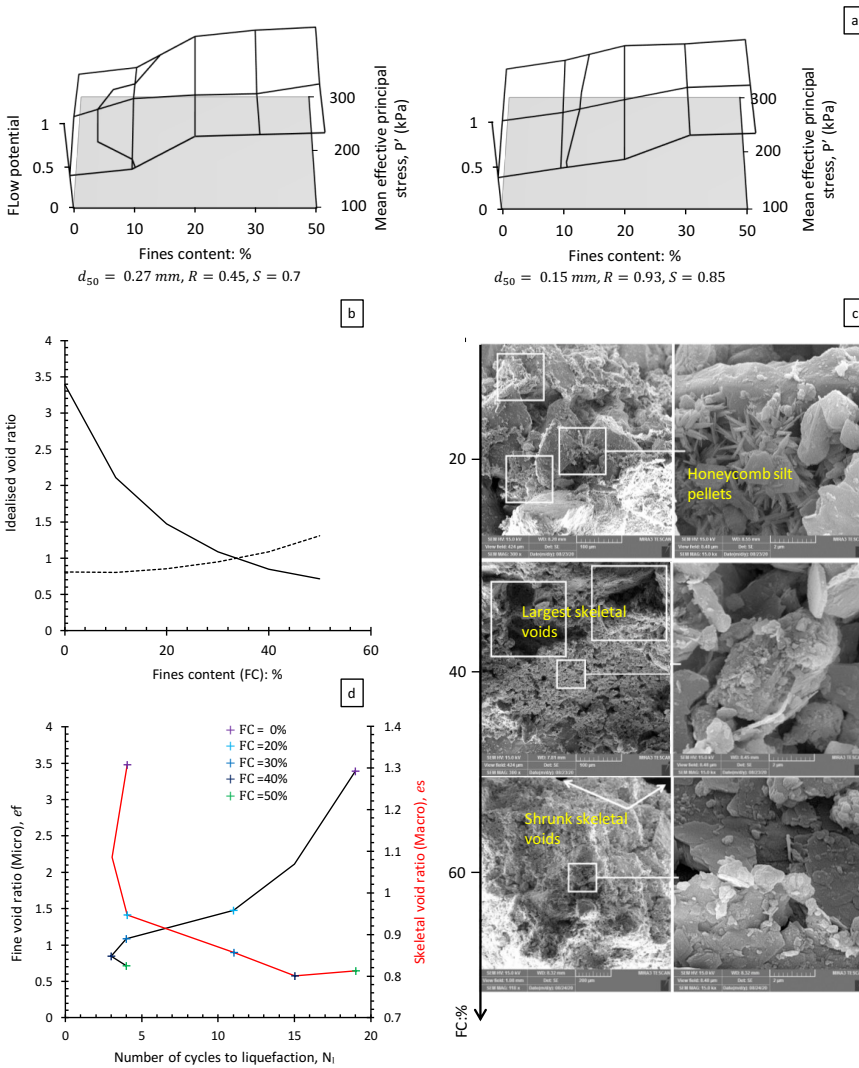
1826

1827

1828

1829

1830 Figure 6



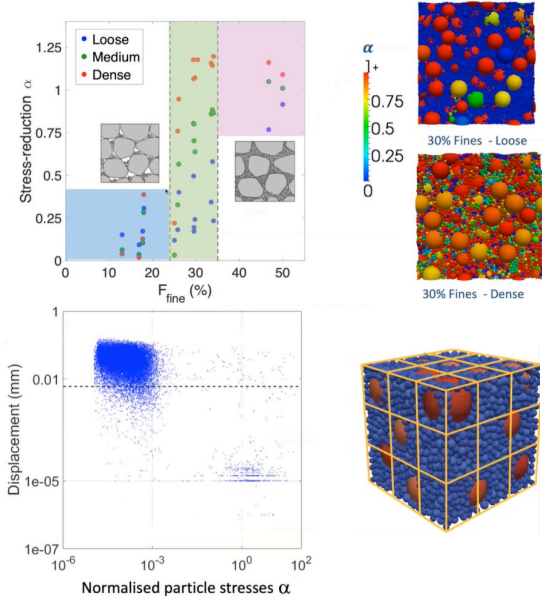
1831

1832

1833

1834

1835 Figure 7



1836

1837

1838

1839

1840

1841

1842

1843

1844

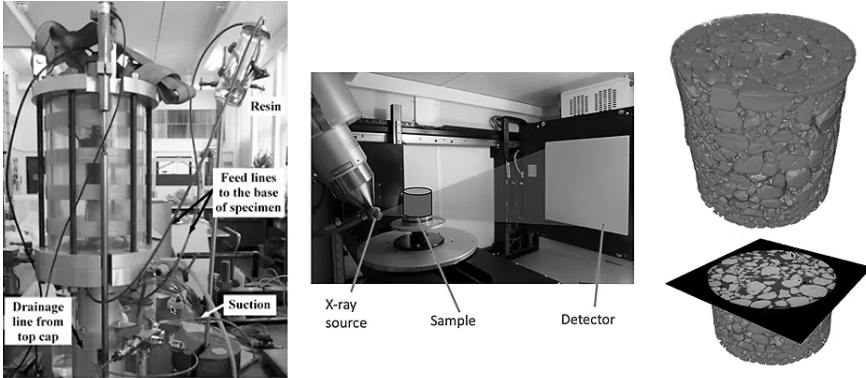
1845

1846

1847

1848

1849 Figure 8



1850

1851

1852

1853

1854

1855

1856

1857

1858

1859

1860

1861

1862

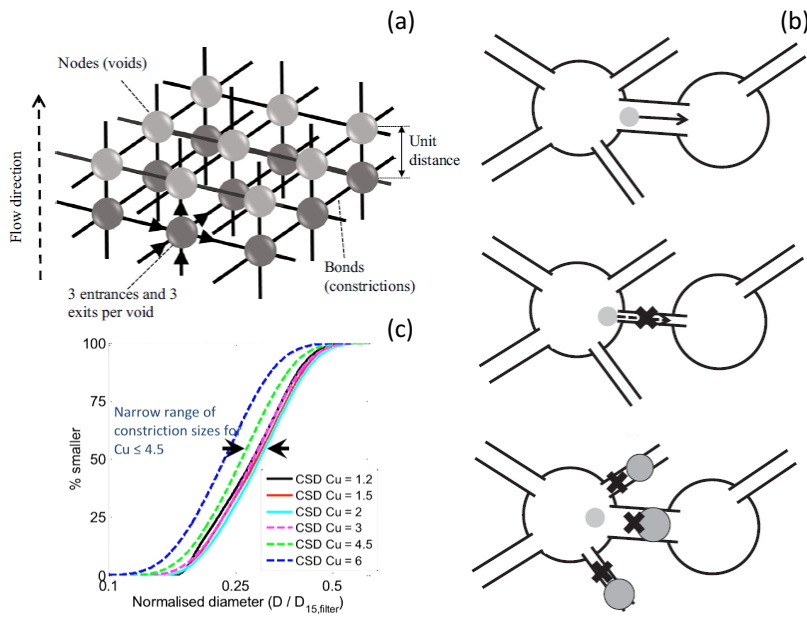
1863

1864

1865

1866

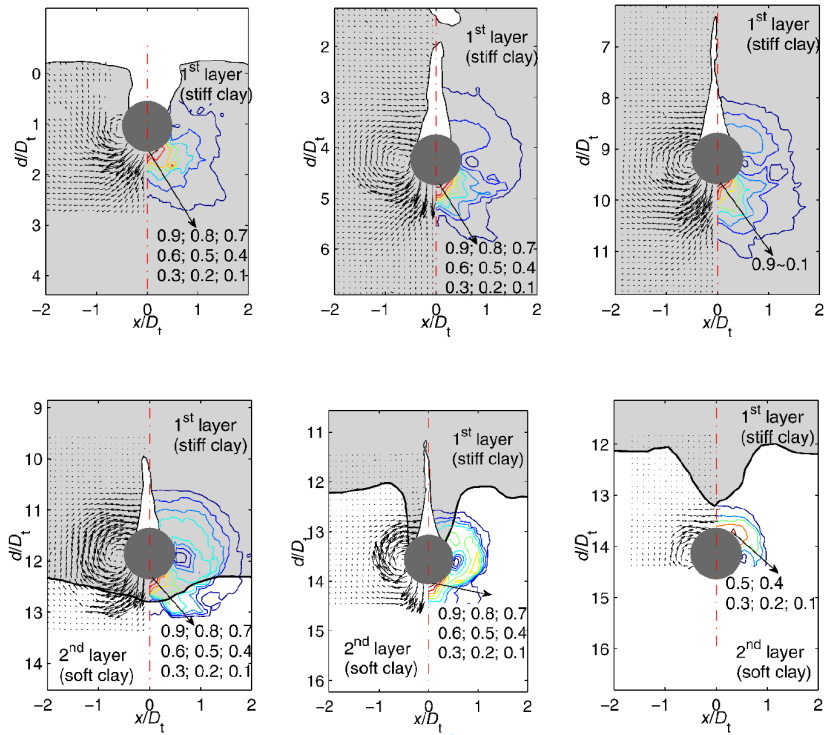
1867 Figure 9



1868  
 1869  
 1870  
 1871  
 1872  
 1873  
 1874  
 1875  
 1876  
 1877  
 1878  
 1879  
 1880



1881 Figure 10



1882

1883

1884

1885

1886

1887

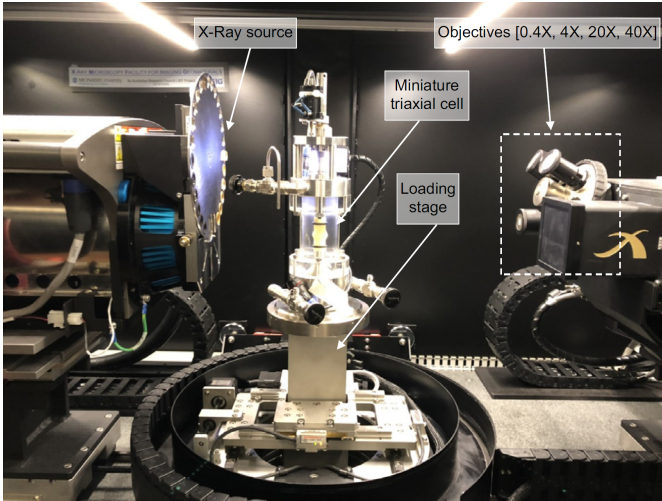
1888

1889

1890

1891

1892 Figure 11



1893

1894

1895

1896

1897

1898

1899

1900

1901

1902

1903

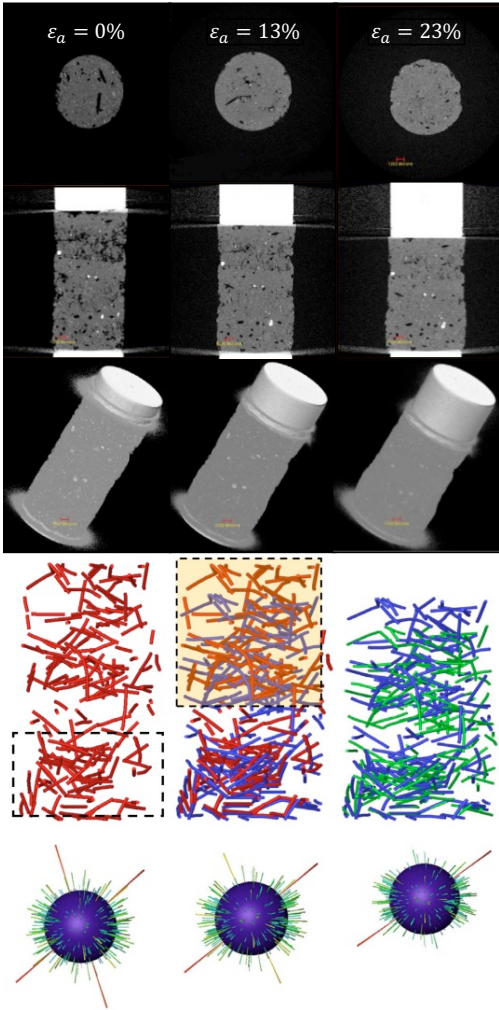
1904

1905

1906

1907

1908 Figure 12



1909

1910

1911

1912

1913

1914

1915 Figure 13

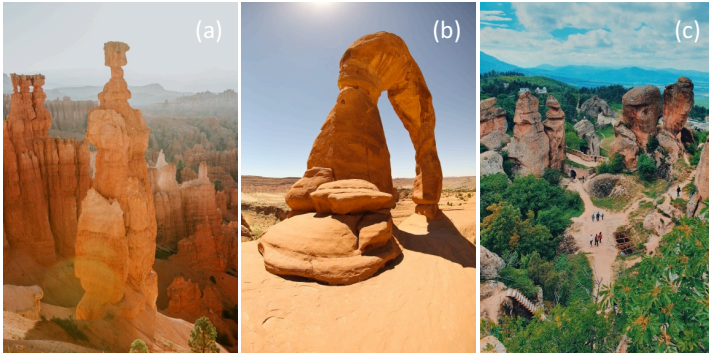


1916

1917

1918

1919 Figure 14



1920

1921

1922

1923

1924

1925

1926

1927

1928

1929

1930

1931

1932

1933

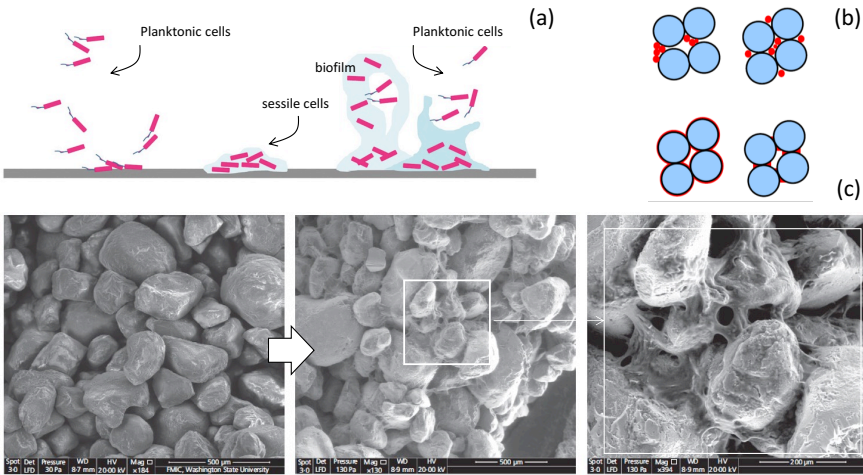
1934

1935

1936

1937

1938 Figure 15



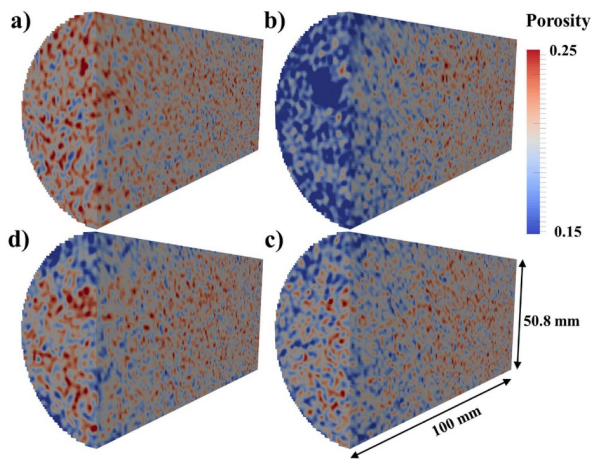
- 1939
- 1940
- 1941
- 1942
- 1943
- 1944
- 1945
- 1946
- 1947
- 1948
- 1949
- 1950
- 1951
- 1952
- 1953

1954 Figure 16



- 1955
- 1956
- 1957
- 1958
- 1959
- 1960
- 1961
- 1962
- 1963
- 1964
- 1965

1966 Figure 17



1967

1968

1969

1970

1971

1972

1973

1974

1975

1976

1977

1978

1979

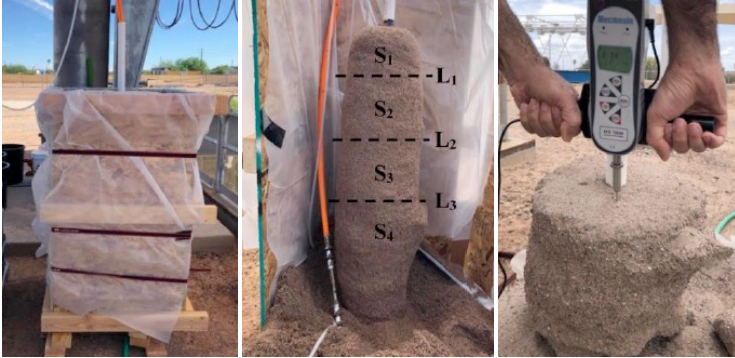
1980

1981

1982



1983 Figure 18



1984

1985

1986

1987

1988

1989

1990

1991

1992

1993

1994

1995

1996

1997

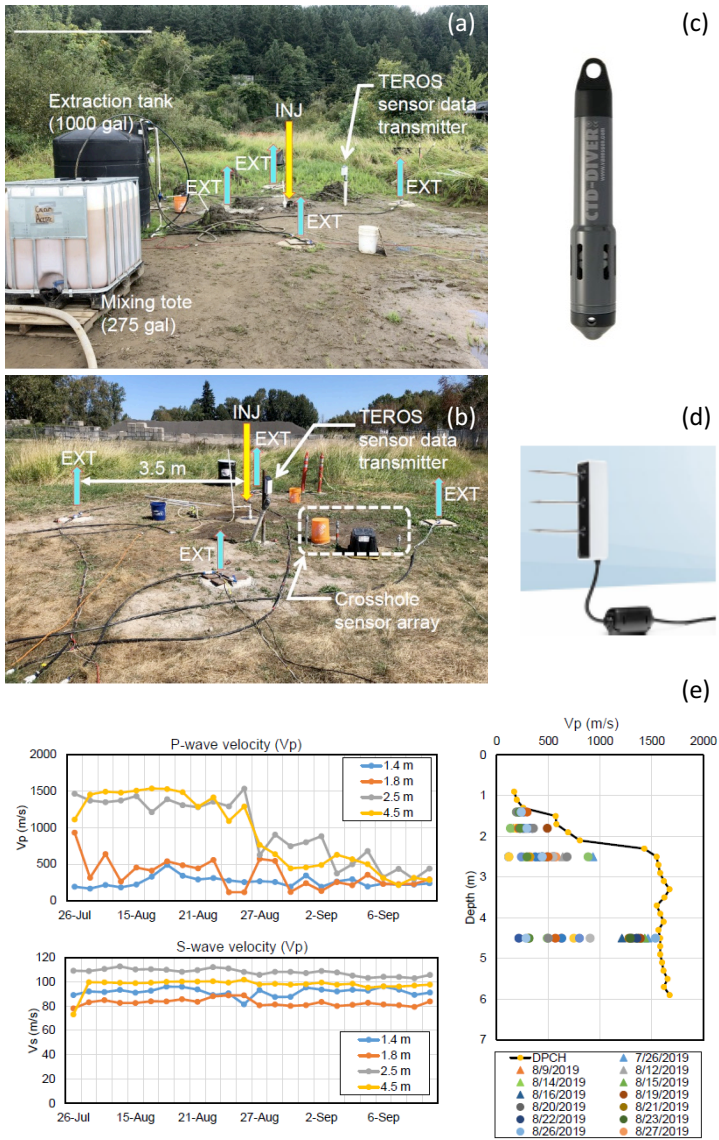
1998

1999

2000

2001

2002 Figure 19

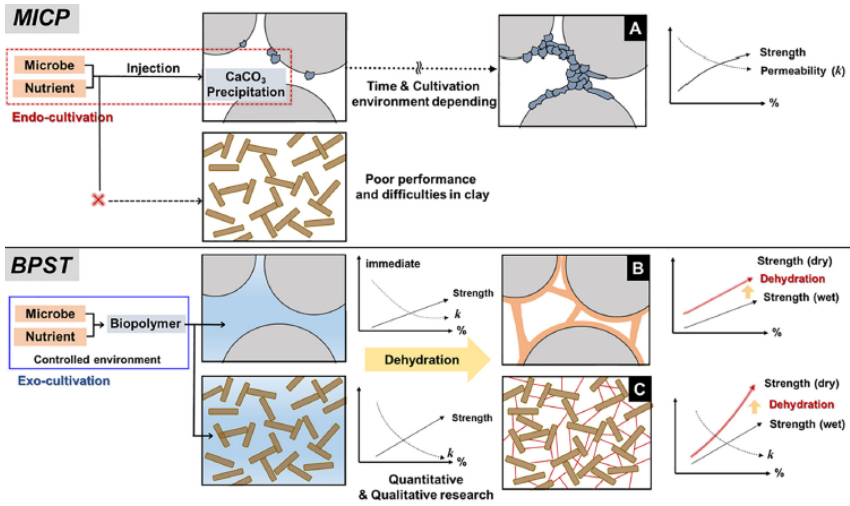


2003

2004

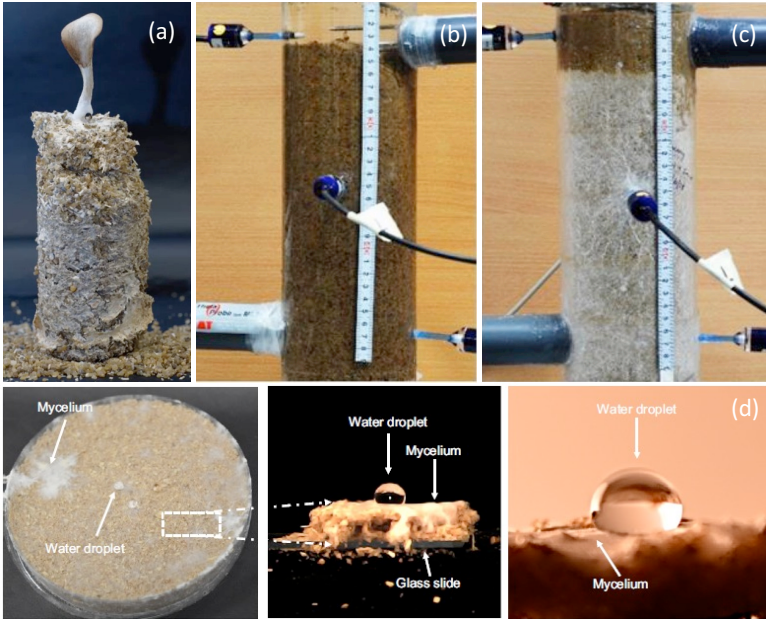
2005

2006 Figure 20



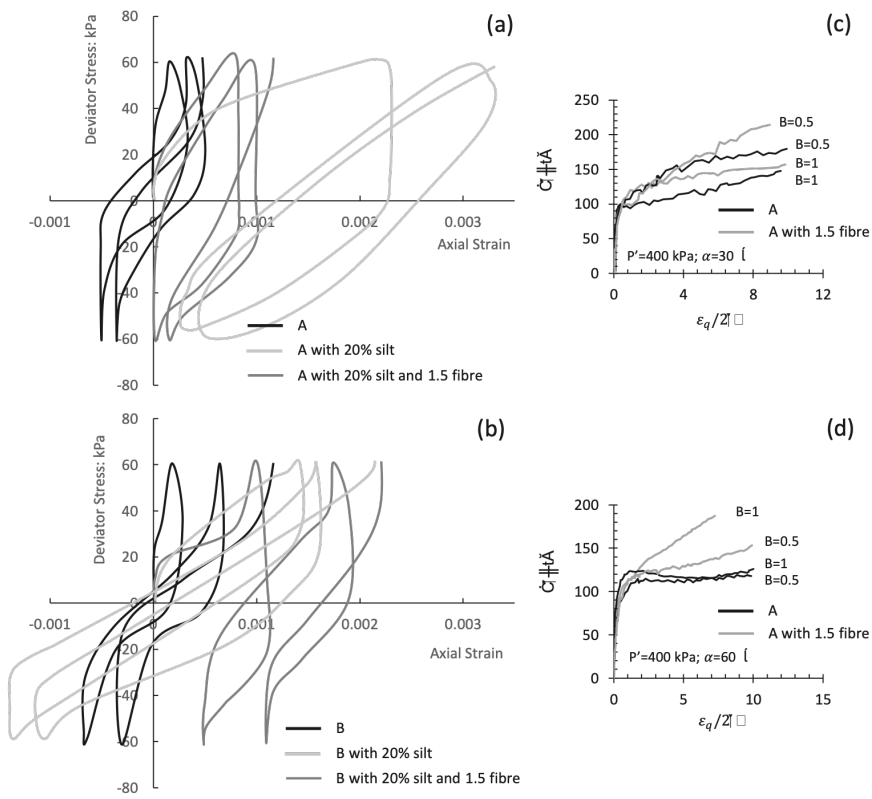
- 2007
- 2008
- 2009
- 2010
- 2011
- 2012
- 2013
- 2014
- 2015
- 2016
- 2017
- 2018
- 2019
- 2020
- 2021

2022 Figure 21



- 2023
- 2024
- 2025
- 2026
- 2027
- 2028
- 2029
- 2030
- 2031
- 2032
- 2033
- 2034
- 2035

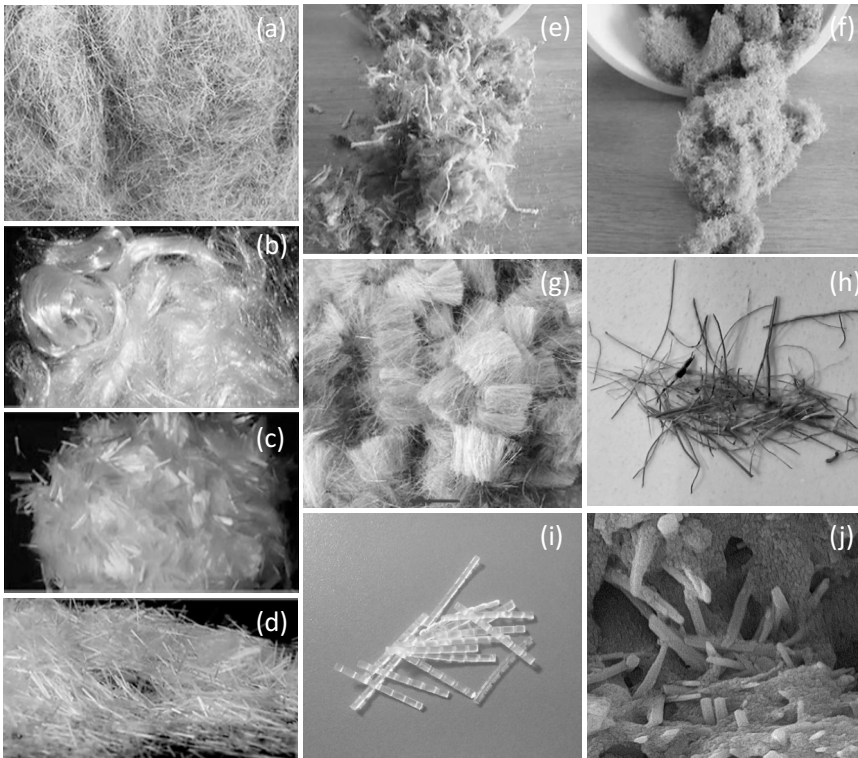
2036 Figure 22



2037  
 2038  
 2039  
 2040  
 2041  
 2042  
 2043  
 2044  
 2045

2046

2047 Figure 23



2048

2049

2050

2051

2052

2053

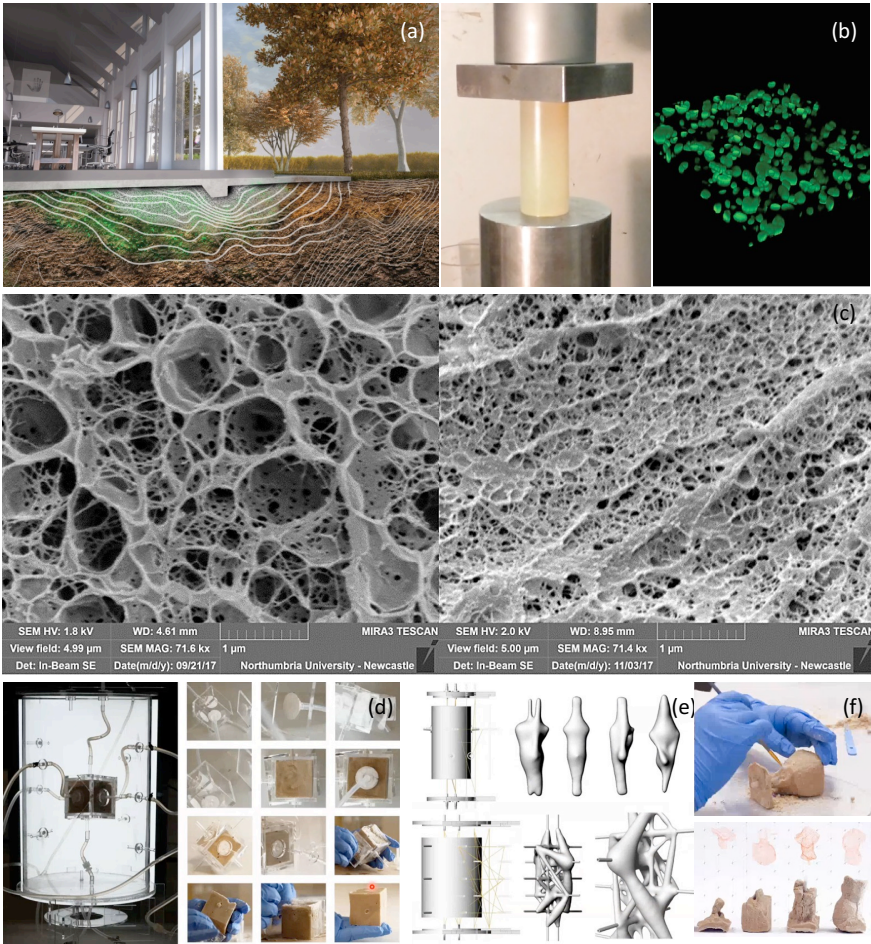
2054

2055

2056

2057

2058 Figure 24



2059